



Connectivity among Photosystem II centers in phytoplankters: Patterns and responses



Kui Xu, Jessica L. Grant-Burt, Natalie Donaher, Douglas A. Campbell*

Department of Chemistry & Biochemistry, Mount Allison University, Sackville, New Brunswick E4L 3M7, Canada

ARTICLE INFO

Keywords:

Fast Repetition and Relaxation chlorophyll fluorescence induction
Light acclimation
Ostreococcus
Photosynthesis
Phytoplankton
Prochlorococcus
Synechococcus
Thalassiosira pseudonana

ABSTRACT

Fast Repetition and Relaxation chlorophyll fluorescence induction is used to estimate the effective absorption cross section of PSII (σ_{PSII}), to analyze phytoplankton acclimation and electron transport. The fitting coefficient ρ measures excitation transfer from closed PSII to remaining open PSII upon illumination, which could theoretically generate a progressive increase in σ_{PSII} for the remaining open PSII. To investigate how ρ responds to illumination we grew marine phytoplankters with diverse antenna structures (*Prochlorococcus*, *Synechococcus*, *Ostreococcus* and *Thalassiosira pseudonana*) under limiting or saturating growth light. Initial ρ varied with growth light in *Synechococcus* and *Thalassiosira*. With increasing actinic illumination PSII closed progressively and ρ decreased for all four taxa, in a pattern explicable as an exponential decay of ρ with increasing distance between remaining open PSII reaction centers. This light-dependent down-regulation of ρ allows the four phytoplankters to limit the effect of increasing light upon σ_{PSII} . The four structurally distinct taxa showed, however, distinct rates of response of ρ to PSII closure, likely reflecting differences in the spacing or orientation among their PSII centers. Following saturating illumination recovery of ρ in darkness coincided directly with PSII re-opening in *Prochlorococcus*. Even after PSII had re-opened in *Synechococcus* a transition to State II slowed dark recovery of ρ . In *Ostreococcus* sustained NPQ slowed dark recovery of ρ . In *Thalassiosira* dark recovery of ρ was slowed, possibly by a light-induced change in PSII spacing. These patterns of ρ versus PSII closure are thus a convenient probe of comparative PSII spacings.

1. Introduction

Photosystem II (PSII) is composed of a reaction center (PSII RC) served by light harvesting complexes, which together absorb light and transform it to chemical energy for reductive assimilation in plants, algae and cyanobacteria. Transfer of excitons from light harvesting complexes to the PSII RC is fast and occurs with a high quantum yield [1–3]. However, the excitons visiting the PSII RC have alternate fates; to be trapped by the PSII RC and thereby induce charge separation, heat dissipation or fluorescence dissipation, or to be transferred to neighboring PSII RC until the exciton is eventually trapped, lost as heat or emitted as fluorescence [4]. The connectivity parameter (ρ) expresses the probability of an exciton visiting one PSII RC and then transferring to another neighboring PSII RC [1,5,6]. The concept of ρ was proposed by Joliot and Joliot 1964 [7] to explain a dampened, non-exponential increase in fluorescence as PSII RC close. ρ can be detected through sigmoidicity of a chlorophyll *a* fluorescence induction curve as PSII centers go from open to closed under the influence of a single turnover saturating flash [1,5,8,9]. ρ has interacting implications for parameters

derived from chlorophyll fluorescence induction curves for algae and cyanobacteria, including how the effective absorption cross section for PSII photochemistry (σ_{PSII}) [5] and the rate of electron transport through PSII [10] will respond to increasing light.

Fast Repetition Rate (FRR) fluorescence can be used to measure ρ , σ_{PSII} and other PSII functional parameters without the addition of inhibitors [5]. Fluorometers based upon the FRR principle apply a train of flashlets to cumulatively and rapidly induce closure of PSII, and are now extensively used in laboratory and field studies to investigate photosynthesis in phytoplankton populations [11–14]. With FRR, the flashlet intensity, number and repeat rate are chosen to provoke only a single reduction of each Q_A site (Q_A) within one flashlet train. This single turnover avoids multiple turnovers of PSII within a given flashlet train [5] that would in turn distort the model assumptions used to extract functional parameters from the fluorescence rise curve.

In an FRR fluorescence induction curve σ_{PSII} is derived as a target size parameterization of the exponential rise of fluorescence towards the maximal fluorescence (F_M) asymptote in response to cumulative photons delivered. ρ is derived from the degree of sigmoidal departure

Abbreviations: ρ , coefficient of excitation transfer among PSII units; σ_{PSII} , effective absorption cross section for Photosynthesis II

* Corresponding author.

E-mail address: dcampbell@mta.ca (D.A. Campbell).

<http://dx.doi.org/10.1016/j.bbambio.2017.03.003>

Received 24 December 2016; Received in revised form 10 March 2017; Accepted 13 March 2017

Available online 14 March 2017

0005-2728/ © 2017 Elsevier B.V. All rights reserved.

from a simple exponential rise curve [1,5]. σ_{PSII} has been widely measured among diverse marine phytoplankton [15,16], and shown to decrease dynamically in response to high light due to non-photochemical quenching (NPQ) [17]. σ_{PSII} increases when phycobilisome excitation shifts from PSI to PSII in cyanobacteria in a state 2 to state 1 transition [18]. Moreover, σ_{PSII} changes in response to stress conditions [15,19] and during acclimation to changing light [20]. According to a simple concept of the effect of ρ , σ_{PSII} measured under actinic light should increase as PSII RC close under the influence of increasing actinic light since the excitons captured by antenna complexes should be transferred from closed PSII to the remaining open PSII, so that average antenna size per open PSII increases. In parallel, however, induction of non-photochemical quenching could act to decrease σ_{PSII} under actinic light. This expected interaction of ρ and σ_{PSII} complicates efforts to analyze changes in σ_{PSII} under the influence of non-photochemical quenching. We therefore sought to characterize interactions of ρ with non-photochemical quenching and with σ_{PSII} in the face of increasing actinic excitation.

We grew four marine phytoplankton taxa with diverse photophysiology and light harvesting antennae systems; a diatom, a prasinophyte, a picocyanobacteria and a *Prochlorococcus* (Table 1) under growth limiting and growth saturating actinic lights. We determined the effects of FRR flashlet intensity on estimated ρ , and established protocols to extract consistent estimates of ρ on suspended phytoplankton cultures. We then measured responses of ρ to increasing actinic light, and the interactions of ρ with σ_{PSII} , yield of non-photochemical quenching (YNPQ) and PSII closure (q_L) across these four species. We sought to determine if the patterns of measured ρ vary across taxa or with growth light. Across the taxa and growth light combinations we sought to determine if ρ interacted with progressive closure of PSII centres to drive an increase in the σ_{PSII} for remaining open PSII centres. This is a critical issue for estimations of PSII electron transport [15,21,22] and of PSII content [23–25] across taxa. Finally, we sought to use the photophysiological diverse phytoplankters to explore general or taxa-specific factors that control or influence changes in measured ρ with increasing actinic light levels

2. Materials and methods

We examined four taxa of marine phytoplankton in this study (Table 1). The cyanobacterial species, *Prochlorococcus marinus* MED4 (*Prochlorococcus*) obtained from Provasoli-Guillard National Center of Marine Phytoplankton (NCMA, Boothbay Harbour Maine) was grown in Pro99 medium prepared using the Pro99 kit from NCMA [31]. *Synechococcus* sp. WH8102 (*Synechococcus*) obtained from NCMA was grown in L1-Si medium [32]. The prasinophyte green algae, *Ostreococcus tauri* RCC745 (*Ostreococcus*) obtained from Roscoff Culture Collection (RCC) was grown in f/2 medium [33] without adding sodium silicate. The marine centric diatom strain *Thalassiosira pseudonana* CCMP1335 (*Thalassiosira*) obtained from the NCMA was cultured in f/2 medium [33]. We grew all four taxa in a temperature controlled incubator at 22 °C and 30 $\mu\text{mol photons m}^{-2} \text{s}^{-1}$ or 260 $\mu\text{mol photons m}^{-2} \text{s}^{-1}$, with a light/dark cycle of 12 h:12 h. We chose these

Table 1

Diameter, major pigments, major light harvesting complex (LHC) and state transition evidence in four phytoplankters.

Species	Diameter	Major pigments	Major LHC	State transition
<i>Prochlorococcus</i>	~0.6 μm	Chl a2, b2 [26]	Pcb	Not in MED4 [27]
<i>Synechococcus</i>	~1 μm	Chl a, APC, APC, PE (PEB & PUB) [57]	PBS	PBS movement, spillover [28]
<i>Ostreococcus</i>	~1 μm	Chl a, b	LHCs	Not found [29]
<i>Thalassiosira</i>	~5 μm	Chl a, c	FCPs	Not found [30]

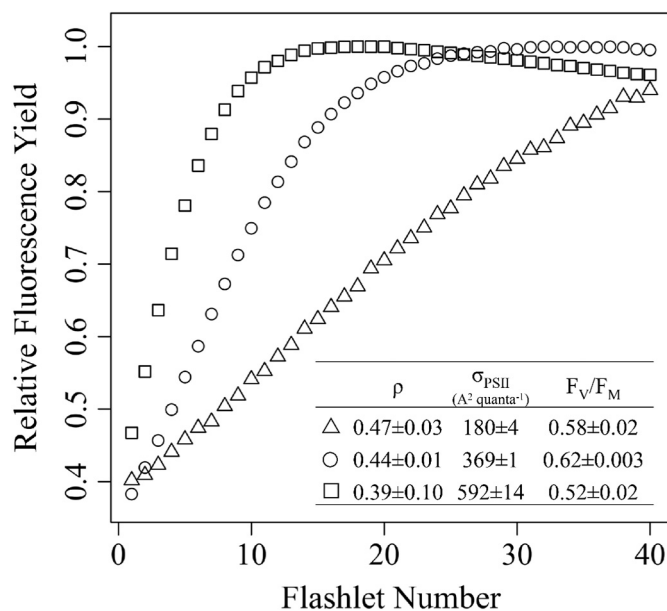


Fig. 1. Representative Chlorophyll Fluorescence Fast Repetition Rate induction curves with different flashlet intensities.

growth light levels based upon our experience as growth limiting or growth saturating light, within the acclimatory range of the four diverse taxa. We tracked the growth of cultures by following fluorescence emission at 680 nm (*Prochlorococcus*, *Ostreococcus* & *Thalassiosira*) or at 650 nm (*Synechococcus*) using a plate spectrofluorometer (SpectraMax Gemini EM, Molecular Devices, Sunnyvale, USA).

When cultures reached mid-exponential phase we took samples for chlorophyll fluorescence induction measurements, placed them in a 2 ml cuvette and then dark-adapted them for ~2 min. Samples were then exposed to a train of 40 blue (455 nm) flashlets with a duration of 1.2 μs separated by an intervening interval of 1.0 μs of darkness to induce a Fast Repetition and Relaxation (FRR) fluorescence induction curve [5], using a Photon Systems Instruments FL3500 fluorometer system (Brno, Czech Republic). This train of 40 blue flashlets cumulatively induced a single turnover of PSII which reduced Q_A and thereby closed PSII. We chose the intensity of the flashlet for each species in order to saturate the fluorescence rise within around 30 of 40 flashlets (Fig. 1) [34,35]. For each FRR induction curve we exported the data from the FluorWin data capture software to fit a model with four parameters: minimal fluorescence, F_0 ; maximal fluorescence, F_M ; effective absorption cross section for PSII photochemistry, σ_{PSII} ; and coefficient of excitonic connectivity ρ ; [5] using the PSIWORX-R package (A. Barnett, sourceforge.net) [25,36]. For each measurement, we did an FRR induction before and then again after a 1 s period of darkness to allow PSII to re-open after illumination. We thus determined in the dark F_0 , F_M , σ_{PSII} , ρ ; under actinic light F_S , F_M' , σ_{PSII}' , ρ' ; and following 1 s of darkness after actinic light $F_0' 1 \text{ s}$, $F_M' 1 \text{ s}$, $\rho' 1 \text{ s}$, $\sigma_{\text{PSII}}' 1 \text{ s}$.

We then estimated F_0' as:

$$F_0' = F_0'_{1s} * \{1 - [(F_M'_{1s} - F_M')/F_M'_{1s}]\}$$

[37].

To examine the response of PSII function to increasing light intensity in the four studied species, we set a series of 60 s exposures to increasing steps of actinic light levels from 0 to a maximal light level. We measured the FRR induction curve at the end of each light level exposure, and then again after 1 s dark period to allow re-opening of PSII. We estimated the coefficient of photochemical quenching (q_L):

$$q_L = (F_M' - F_S)/(F_M' - F_0') * (F_0'/F_S)$$

[38].

We estimated the yield of non-photochemical quenching (YNPQ):

$$\text{YNPQ} = F_S/F_M' - F_S/F_M$$

[39],

We followed Serôdio et al. [40] and used the maximum value of F_M attained for a given sample, not necessarily the value measured after initial dark acclimation, as our basis for estimation of YNPQ.

We calculated the electron transport rate as:

$$\text{ETR} (\text{e}^- \text{PSII}^{-1} \text{s}^{-1}) = \sigma_{\text{PSII}} (\text{or } \sigma_{\text{PSII}}') * q_L * E$$

[15].

Where E is actinic irradiance ($\mu\text{mol photons m}^{-2} \text{s}^{-1}$). We calculated ETR using $\sigma_{\text{PSII}}'1 \text{ s}$ because σ_{PSII}' could not be estimated reproducibly under high actinic light in *Ostreococcus* grown under $260 \mu\text{mol photons m}^{-2} \text{s}^{-1}$, and we did not find any significant difference between σ_{PSII}' and $\sigma_{\text{PSII}}'1 \text{ s}$ in the other three study species. Further details of the definitions of fluorescence variables and parameters are in S1 Table.

Using the light response curves, we chose the lowest actinic light sufficient to drive ρ to a minimal level in each species. This actinic light intensity was then used to examine the recovery of ρ after light exposure in the four studied species. For the ρ recovery measurement protocol we set an initial dark period of 10 s and measured the FRR induction at the end of the dark period to get the initial dark ρ in the four studied species. Then we applied 4 sequential periods of 10 s of the saturating actinic light appropriate for each species from each growth light level, with an FRR measurement every 10 s, to track the decrease of ρ to a minimal level under saturating actinic light. Each FRR measurement applied a saturating flashlet series to the illuminated cells and then another saturating flashlet series after 1 s of darkness. Then we turned off the saturating light and tracked ρ recovery under darkness with an FRR measurement every 10 s, for a total of 50 s. To examine the effects of state transitions, a component of measured non-photochemical quenching [41], on ρ recovery in *Synechococcus*, we repeated the ρ induction and recovery experiment but provided low light, instead of darkness to cultures during the recovery phase to inhibit any state 1 to state 2 transition that occurred under darkness.

Two way ANOVA followed by Tukey's honestly significantly difference (Tukey's HSD) test was conducted to test the statistical significance of the differences among means of initial ρ across the species grown under two light intensities. Further details of statistical analyses are provided in figure legends and in S2 Statistical Results.

3. Results

3.1. Selection of FRR flashlet intensity and initial ρ values

Fig. 1 presents representative effects of FRR flashlet intensity on fluorescence induction patterns and therefore upon estimated excitation transfer among PSII units (ρ). Excessive flashlet intensity leads to rapid saturation of chlorophyll fluorescence emission within a few flashlets. This leads to an under-estimate of ρ (0.39 in the example Fig. 1) with a wide confidence interval (0.10) using the PSIWORX-R (www.sourceforge.net) fitting routine. In contrast, insufficient flashlet intensity leads to a failure to fully saturate chlorophyll fluorescence emission by the end of the 40 flashlets applied. This leads to an over-estimate of ρ (0.47 in the example Fig. 1) with a large confidence interval (0.03). The third scenario in Fig. 1 is observed when full saturation occurred at flashlet number ~ 30 of the 40 applied flashlets [34,35] with an intermediate ρ value (0.44 in the example Fig. 1) with a small confidence interval (0.01). This same saturation profile gave the highest estimated value and smallest confidence interval for F_V/F_M and the smallest confidence interval on the estimate for σ_{PSII} . We did similar tests for all species grown at 30 or 260 $\mu\text{mol photons m}^{-2} \text{s}^{-1}$ to select the lowest flashlet intensity sufficient to drive the samples to saturation within ~ 30 flashlets, to achieve the smallest confidence intervals on estimates of ρ and σ_{PSII} and the maximal estimates for F_V/F_M .

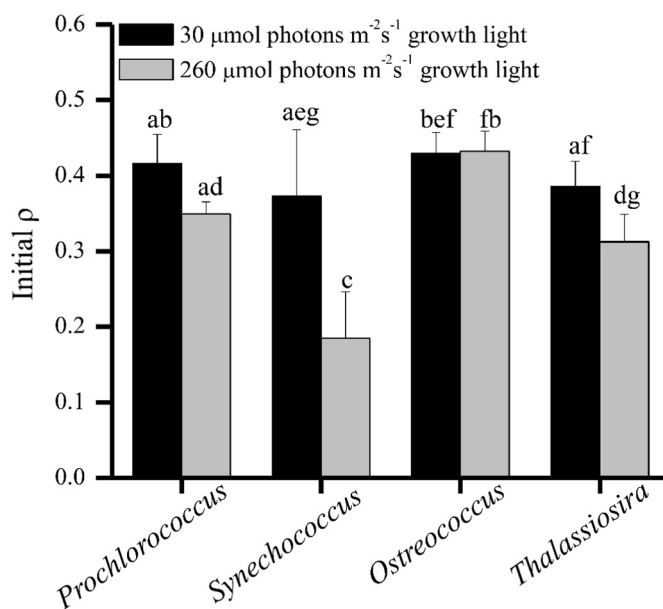


Fig. 2. The initial dark-acclimated ρ for four phytoplankters. Cultures were grown under limiting (dark columns) or saturating light (lighter columns). Bars sharing a common letter were not significantly different from one another (Tukey's HSD, $P < 0.05$). $n = 4-6$ independently grown cultures, means \pm S.D.

The symbols show measurement points from Fast Repetition Rate induction curves provoked by a series of 40 flashlets (1.2 μs duration, 2 μs intervening dark) applied over 128 μs that cumulatively closed Photosystem II. Triangles, lowest flashlet intensity; circles, intermediate flashlet intensity; squares, highest flashlet intensity. These sample curves were taken from a sample of *Prochlorococcus* MED4 grown under $30 \mu\text{mol photons m}^{-2} \text{s}^{-1}$. The inset table shows parameter and 95% confidence interval estimates from curve fits of the induction curves.

The initial dark-acclimated ρ measured for the four phytoplankton species after growth under limiting or saturating light is presented in Fig. 2. ρ was significantly lower in *Synechococcus* and *Thalassiosira* grown under saturating light compared to growth under limiting light. ρ was lowest in *Synechococcus* (0.18) while it was highest in *Ostreococcus* (0.43), in both cases for cultures grown under saturating light. *Synechococcus* showed wider variation among replicate determinations of ρ , possibly because its large state transitions generated strongly time-dependent scatter among the replicates during transfer from growth to measurement conditions.

3.2. *Prochlorococcus* connectivity and Photosystem II function

Fig. 3 presents the responses of Photosystem II to increasing actinic irradiance in *Prochlorococcus*, with parameters (S1 Table) extracted from FRR chlorophyll fluorescence induction curves (Fig. 1) measured under a series of increasing actinic irradiance levels. For cultures from growth limiting $30 \mu\text{mol photons m}^{-2} \text{s}^{-1}$ the dark-acclimated initial ρ (0.42) decreased to minimal levels once actinic irradiance reached $65 \mu\text{mol photons m}^{-2} \text{s}^{-1}$. Estimated ρ' then increased as the irradiance increased above saturating levels (Fig. 3A). These estimates under high actinic light showed high variability and wide confidence intervals on the parameter estimates from individual FRR curves, because the amplitude of variable fluorescence remaining above steady state fluorescence was small. In further analyses, we therefore focused on the initial decline in ρ' as irradiance increases from darkness to saturating levels. After exposure of cultures from growth limiting light to $65 \mu\text{mol photons m}^{-2} \text{s}^{-1}$, $\rho'1 \text{ s}$ recovered to 73% of the initial dark value (Fig. 3B). This $\rho'1 \text{ s}$ recovery decreased after exposure to yet higher light intensities (Fig. 3B). For cultures from growth saturating $260 \mu\text{mol photons m}^{-2} \text{s}^{-1}$ (Fig. 3A) the starting dark acclimated ρ was

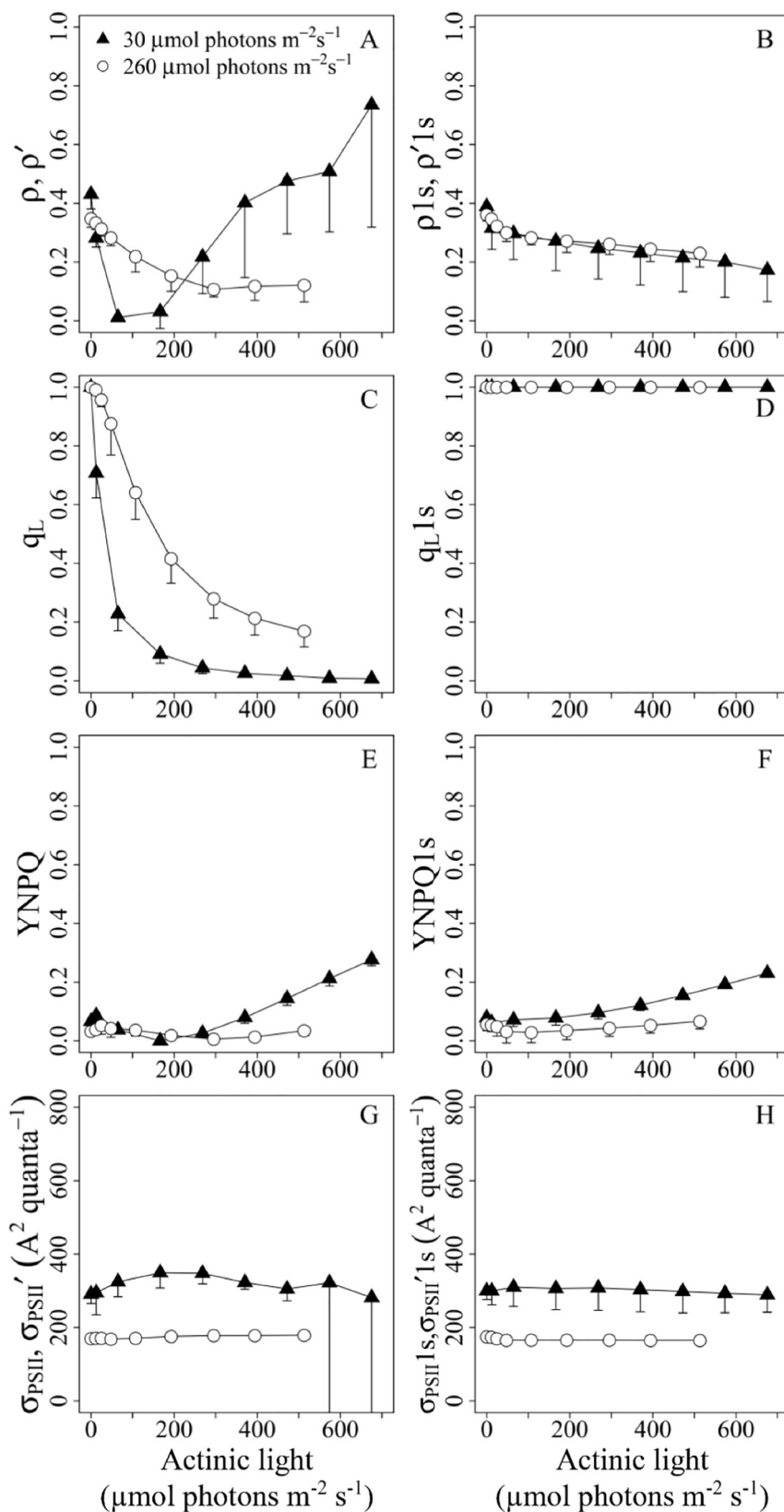


Fig. 3. Responses of Photosystem II to increasing light intensity in *Prochlorococcus*. Cultures from growth limiting (filled triangles) or growth saturating light (empty circles); $n = 4-8$ independently grown cultures, means \pm S.D. (A) Coefficient of excitation transfer among PSII units under actinic light (ρ') or (B) after 1 s dark following actinic light ($\rho'1s$). (C) Coefficient of photochemical quenching under actinic light (q_L) or (D) after 1 s dark following actinic light (q_L1s). (E) Yield of non-photochemical quenching under actinic light (YNPQ) or (F) after 1 s dark following actinic light (YNPQ1s). (G) Effective absorption cross section for PSII photochemistry under actinic light (σ_{PSII}) ($A^2 \text{ quanta}^{-1}$) or (H) after 1 s dark following actinic light ($\sigma_{PSII}1s$).

lower (0.35). ρ then decreased to a minimal level by an irradiance of $295 \mu\text{mol photons m}^{-2} \text{s}^{-1}$. q_L [38] decreased faster and reached a lower level with increasing irradiance in cultures from growth limiting light, compared to cultures from growth saturating light (Fig. 3C). q_L 1 s completely recovered to 1 (Fig. 3D). In cultures from growth limiting light YNPQ reached 0.27 when light intensity reached $675 \mu\text{mol photons m}^{-2} \text{s}^{-1}$; after 1 s dark, YNPQ relaxed back to 0.23 (Fig. 3F). In *Prochlorococcus* from growth saturating light a fraction of the PSII pool remained open even under high light (Fig. 3C) and we did not detect any evidence of induction of YNPQ (Fig. 3E and F). For cultures from growth limiting light σ_{PSII} (Fig. 3G) increased as irradiance increased from 0 to $167 \mu\text{mol photons m}^{-2} \text{s}^{-1}$. After only 1 s dark, σ_{PSII} 1 s recovered to the initial value after all treatment light levels (Fig. 3H). In contrast for cultures from growth saturating light there was no effect of measurement light upon σ_{PSII} nor upon σ_{PSII} 1 s (Fig. 3G and H). σ_{PSII} was significantly higher in the cells from growth limiting than in cells from growth saturating light. An increase in YNPQ related to antenna processes (Fig. 3E) would be expected to provoke a decrease in σ_{PSII} (Fig. 3G). We therefore attribute the rise in measured YNPQ in cultures from growth limiting light (Fig. 3E) to non-photochemical quenching outside the antennae.

We plotted the electron transport rate (ETR) response to increasing light for *Prochlorococcus* (Fig. 4A). Maximal electron transport rate (ETR_{max}) and the light level for saturation of ETR (I_K) were both higher in *Prochlorococcus* from growth saturating light compared to cultures from growth limiting light (Table 2). In an even array of PSII centers, the reciprocal of the fraction of open PSII RC, $1/q_L$ will be directly proportional to the distance between remaining open PSII RC. Since ρ should depend upon the distance to the next available open PSII RC (M. Gorbunov, pers. comm.) we plotted ρ versus $1/q_L$ for *Prochlorococcus* (Fig. 4B) using the data from Fig. 3A, C. For Fig. 4B, we considered only those paired points of ρ and $1/q_L$ taken as irradiance increased from 0 to saturating levels (Fig. 4A), and not those points with low confidence taken under excess light (Fig. 3A). We found that a single phase exponential decay described the relation between ρ versus $1/q_L$ for data pooled from *Prochlorococcus* from growth limiting or growth saturating light.

Fig. 5 presents kinetic changes in Photosynthesis II function in *Prochlorococcus* under saturating light and subsequent dark recovery. Cultures were initially measured after dark acclimation (60 s), then exposed to $167 \mu\text{mol photons m}^{-2} \text{s}^{-1}$ (for cultures grown at limiting $30 \mu\text{mol photons m}^{-2} \text{s}^{-1}$) or to $365 \mu\text{mol photons m}^{-2} \text{s}^{-1}$ (for cultures grown at saturating $260 \mu\text{mol photons m}^{-2} \text{s}^{-1}$) for 4×10 s with an FRR measurement every 10 s. This was in each case sufficient to saturate the light-induced down-regulation of ρ' (Fig. 3A). Cultures were then shifted back to darkness for recovery. ρ and q_L decreased to minimal levels within 10 s under the saturating light treatment but completely recovered within the first 10 s of dark recovery period (Fig. 5A and B). Comparing Fig. 5A with Fig. 3B we see that after down-regulation induced by exposure to saturating light measured ρ partially recovers within 1 s (Fig. 3B) and completely recovers by 10 s (Fig. 5A). YNPQ was not induced by the saturating light treatments in *Prochlorococcus* grown under either light condition (Fig. 5C). σ_{PSII} fluctuated slightly but showed limited response to the light or subsequent dark recovery (Fig. 5D), although as in Fig. 3GH σ_{PSII} was significantly higher in *Prochlorococcus* cells from growth limiting than in cells from growth saturating light.

3.3. *Synechococcus* connectivity and Photosystem II function

For *Synechococcus* cultures from growth limiting light the dark-acclimated initial ρ (0.44) decreased to minimal levels once actinic irradiance reached $370 \mu\text{mol photons m}^{-2} \text{s}^{-1}$ (Fig. 6A) but ρ 1s thereafter recovered to 75% of the initial dark value (Fig. 6B). For cultures from growth saturating light (Fig. 6A) the dark acclimated initial ρ was significantly lower (0.24). ρ' increased under $65 \mu\text{mol}$

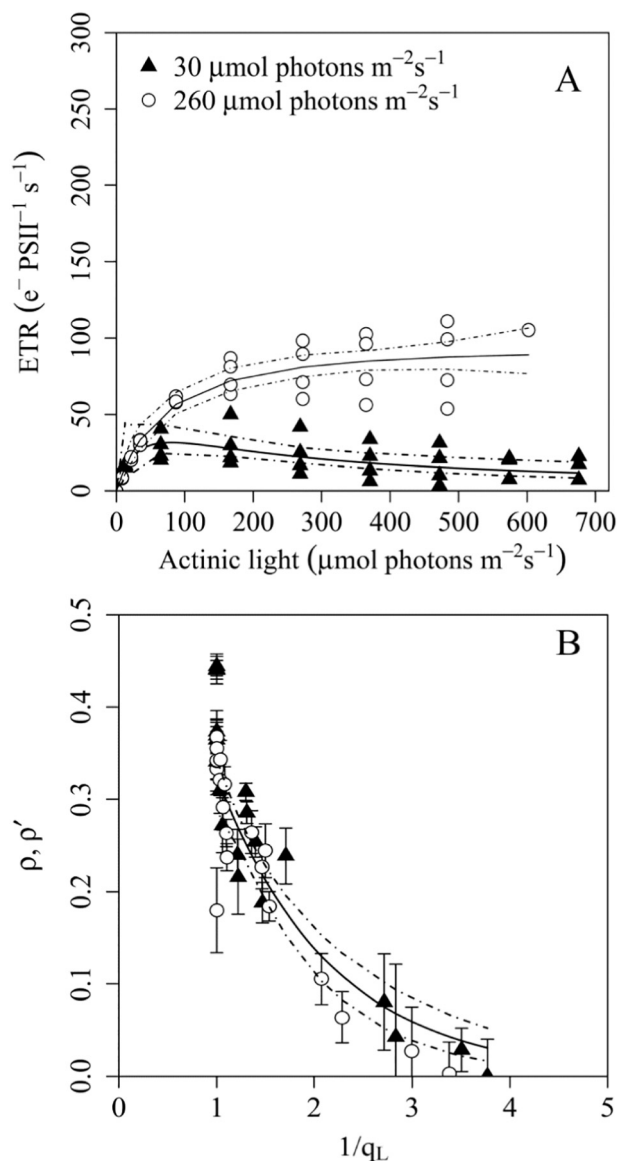


Fig. 4. Light response curves of *Prochlorococcus*. (A) Electron transport rate (ETR) response to increasing light. Cultures from growth limiting (filled triangles) or growth saturating light (empty circles) were fit according to the equation $\text{ETR} = E / (a \times E^2 + b \times E + c)$ [42,43]; dotted lines show 95% confidence interval of the regression lines. Fitting data from the two growth lights separately gave a significantly better fit than a common fit of all data pooled ($F = 64.45$, $P < 0.05$). $n = 4$ independently grown cultures, means \pm S.D. (B) Coefficient of excitation transfer among PSII units (ρ, ρ') plotted against the reciprocal of simultaneously determined coefficient of photochemical quenching ($1/q_L$). Cultures were exposed to 0 to $167 \mu\text{mol photon m}^{-2} \text{s}^{-1}$ (filled triangles) 0 to $365 \mu\text{mol photons m}^{-2} \text{s}^{-1}$ (open circles). Error bars on ρ determinations show the 95% confidence interval on the fitted parameter from an individual measurement. A nonlinear regression line was fit to the data pooled from both growth lights according to the equation $\rho = a \times \exp.(-b \times (1/q_L))$ ($r^2 = 0.91$, Summed square of residuals = 0.03, Residual standard error = 0.24, Exponential decay rate = 0.85). Black dotted lines show 95% confidence interval of the regression line. Fitting data from the two growth lights separately did not show a significantly better fit than a common fit of all data pooled ($F = 2.16$, $P > 0.05$). $n = 4$ independently grown cultures, means \pm S.D.

$\text{photons m}^{-2} \text{s}^{-1}$, decreased to a minimal level by an irradiance of $1184 \mu\text{mol photons m}^{-2} \text{s}^{-1}$, and then increased with further increases in irradiance, with increasing scatter among replicates. ρ 1s recovered to 79% of the initial dark value (Fig. 6B). q_L decreased faster and reached a lower level with increasing irradiance in cultures from growth limiting light, compared to cultures from growth saturating light (Fig. 6C), while q_L 1 s completely recovered to 1 (Fig. 6D). In cultures

Table 2

Photophysiological parameters.

Growth rate (μ , d^{-1}), maximal PSII photochemical yield (F_v/F_m), maximal PSII electron transport rate (ETR_{max} , $e^- PSII^{-1} s^{-1}$), saturation threshold light level (I_k , μmol photons $m^{-2} s^{-1}$) and maximal YNPQ for taxa from growth limiting 30 or growth saturating 260 μmol photons $m^{-2} s^{-1}$. $n = 4-8$ independently grown cultures, means \pm S.D.

Species	Growth light	μ	F_v/F_m	ETR_{max}	I_k	Maximal YNPQ
<i>Prochlorococcus</i>	30	NA	0.63 \pm 0.02	~31	~20	0.27
	260	0.36 \pm 0.03	0.59 \pm 0.01	~90	~64	0.04
<i>Synechococcus</i>	30	0.21 \pm 0.08	0.26 \pm 0.02	~239	~135	0.22
	260	0.36 \pm 0.10	0.2 \pm 0.12	~369	~300	0.29
<i>Ostreococcus</i>	30	0.21 \pm 0.03	0.56 \pm 0.03	~279	~61	0.32
	260	0.53 \pm 0.03	0.56 \pm 0.03	~358	~105	0.64
<i>Thalassiosira</i>	30	0.19 \pm 0.02	0.62 \pm 0.02	~140	~36	0.26
	260	0.29 \pm 0.04	0.57 \pm 0.02	~231	~72	0.58

from growth limiting light YNPQ dropped sharply upon illumination, reflecting a State 2 to State 1 transition [41] and was not re-induced with increasing light intensities (Fig. 6E). In *Synechococcus* from growth saturating light YNPQ also decreased from darkness to the first actinic light level and then re-increased when light intensity reached 2100 μmol photons $m^{-2} s^{-1}$ (Fig. 6E), showing some capacity for induction of NPQ under high light [44]. For cultures from growth limiting light σ_{PSII}' (Fig. 6G) increased from 279 to 374 A^2 as irradiance increased from 0 to 675 μmol photons $m^{-2} s^{-1}$. For cultures from growth saturating light σ_{PSII}' increased in parallel with the state 2 to state 1 transition induced by the first actinic light and then decreased in parallel with the induction of YNPQ (Fig. 6G). σ_{PSII}' 1 s showed little response to increasing light level (Fig. 6H).

Maximal electron transport rate (ETR_{max}) and the light level for saturation of ETR (I_k) were higher in *Synechococcus* grown under 260 μmol photons $m^{-2} s^{-1}$ compared to cultures grown under 30 μmol photons $m^{-2} s^{-1}$ (Fig. 7A, Table 2). As with *Prochlorococcus* we found that a single phase exponential decay described the relation between ρ versus $1/q_L$ in *Synechococcus* but the cultures from growth limiting light had a fit distinct from the cultures from growth saturating light (Fig. 7B). To achieve the single phase exponential fit we excluded the measures taken under 0 μmol photons $m^{-2} s^{-1}$ which fell below the trend because of the state 2 to state 1 transition (Fig. 6E).

ρ and q_L decreased to minimal levels within 10 s under the saturating light treatment but completely recovered within the first 10 s of dark recovery period in *Synechococcus* (Fig. 8A and B). YNPQ was induced to 0.16 by the saturating light treatment in *Synechococcus* from growth limiting light and to 0.2 for cultures from growth saturating light (Fig. 8C). As in Fig. 6GH σ_{PSII} was significantly higher in *Synechococcus* from growth limiting than from growth saturating light, but showed limited response to the saturating light or subsequent dark recovery (Fig. 8D).

The effect of state transitions on ρ recovery in *Synechococcus* is shown in Fig. 9. After down regulation under saturating light ρ recovery is faster under low light, with cells maintained in State I with higher σ_{PSII} (Fig. 9A, B) compared to ρ recovery under dark where cells fell back to State II with down-regulation of σ_{PSII} (Fig. 9B). We plotted paired data from Fig. 9A and B from the recovery period following exposure to saturating light and found a linear correlation between ρ and σ_{PSII} (Fig. 9C).

3.4. *Ostreococcus* connectivity and Photosystem II function

For cultures from growth limiting light the dark-acclimated initial ρ (0.44) decreased to minimal levels once actinic light reached 166 μmol photons $m^{-2} s^{-1}$ (Fig. 10A). Thereafter ρ 1 s recovered to only 52% of the initial dark value (Fig. 10B). For cultures from growth saturating light (Fig. 10A) ρ' decreased to a minimal level by an irradiance of 166 μmol photons $m^{-2} s^{-1}$. ρ' 1 s thereafter recovered to only 34% of the initial dark value (Fig. 10B). q_L decreased faster and reached a lower level with increasing irradiance in cultures from growth limiting

light compared to cultures from growth saturating light, (Fig. 10C) but in both cases q_L s completely recovered to 1 (Fig. 10D). In cultures from growth limiting light YNPQ was induced with increasing actinic light, but the induction of YNPQ was much bigger in *Ostreococcus* from growth saturating light (Fig. 10E). For cultures from growth limiting light σ_{PSII}' (Fig. 10G) decreased from 605 to 347 A^2 as irradiance increased from 0 to 272 μmol photons $m^{-2} s^{-1}$, but σ_{PSII}' 1 s then recovered to 522 A^2 (Fig. 10H). For cultures from growth saturating light σ_{PSII}' decreased from 597 to 347 A^2 as irradiance increased from 0 to 272 μmol photons $m^{-2} s^{-1}$, but σ_{PSII}' 1 s only recovered to 404 A^2 (Fig. 10H), with a significant down-regulation of σ_{PSII}' sustained beyond 1 s of dark in parallel with the strong induction of YNPQ.

When we plotted the ETR response to increasing light for *Ostreococcus* (Fig. 11A) we found Maximal electron transport rate (ETR_{max}) and the light level for saturation of ETR (I_k) were higher in this algae from growth saturating light (Table 2) although scatter in our estimates of σ_{PSII}' for *Ostreococcus* led to high variability among replicates in our estimates of ETR. In Fig. 11B we again plotted ρ vs. $1/q_L$ as irradiance increased from 0 to saturating levels (Fig. 11A). We again found that a single phase exponential decay described the relation between ρ and $1/q_L$ for *Ostreococcus*, whether grown under growth limiting or saturating light.

ρ and q_L both decreased to minimal levels under the saturating light treatment but only q_L completely recovered within the first 10 s of dark recovery period (Fig. 12A and B), with a slower recovery in ρ . YNPQ was induced to 0.22 in *Ostreococcus* grown under 30 μmol photons $m^{-2} s^{-1}$ and to 0.46 by in *Ostreococcus* grown under 260 μmol photons $m^{-2} s^{-1}$ (Fig. 12C). σ_{PSII}' decreased under the light treatment and gradually recovered to the initial value under the subsequent dark period (Fig. 12D).

3.5. *Thalassiosira pseudonana* connectivity and Photosystem II function

For cultures from growth limiting light, the dark-acclimated initial ρ (0.39) decreased to minimal levels once actinic irradiance reached 483 μmol photons $m^{-2} s^{-1}$ (Fig. 13A). Thereafter ρ 1 s recovered to only 31% of the initial dark value. For cultures from growth saturating light (Fig. 13A) the starting dark acclimated ρ was lower (0.33) and then decreased to a minimal level by an irradiance of 272 μmol photons $m^{-2} s^{-1}$. ρ' 1 s thereafter recovered to 64% of the initial dark value (Fig. 13B). q_L decreased faster and reached a lower level with increasing irradiance in cultures from growth limiting light compared to cultures from growth saturating light (Fig. 13C). q_L s completely recovered to 1 (Fig. 13D). YNPQ was induced to a higher maximum in cultures from growth saturating light (Fig. 13E). For cultures from growth limiting light σ_{PSII}' (Fig. 13G) increased from 365 under darkness to 399 A^2 under 21 μmol photons $m^{-2} s^{-1}$ but then gradually decreased to 356 A^2 as irradiance increased further.

We plotted the ETR response to increasing light for *Thalassiosira* (Fig. 14A). Maximal electron transport rate (ETR_{max}) and the light level for saturation of ETR (I_k) were higher in *Thalassiosira* from growth

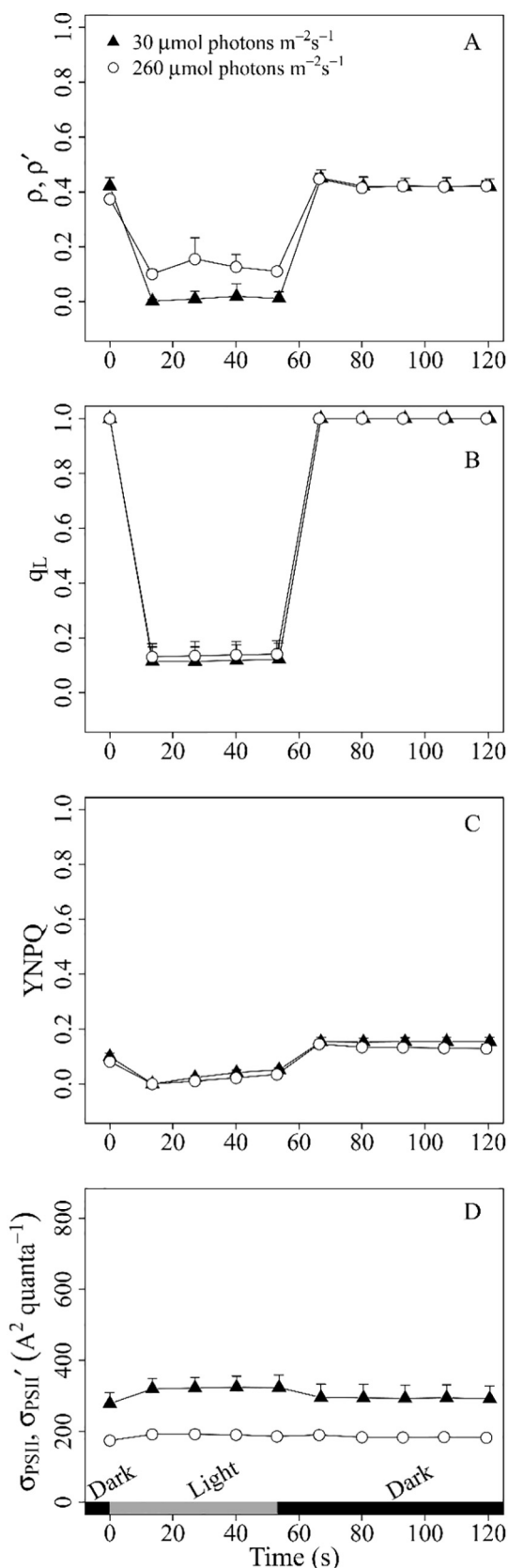


Fig. 5. Changes in Photosystem II function under initial darkness, saturating actinic light and subsequent dark recovery in *Prochlorococcus*. Cultures were measured in darkness (0 s), exposed to saturating light and shifted back to darkness. $n = 4$ independently grown cultures, means \pm S.D. (A) Coefficient of excitation transfer among PSII units (ρ or ρ') (B) Coefficient of photochemical quenching (q_L). (C) Yield of non-photochemical quenching (YNPQ). (D) The effective absorption cross section for PSII (σ_{PSII} or σ_{PSII}' ; $\text{A}^2 \text{ quanta}^{-1}$).

saturating light (Table 2). In Fig. 14B we again plotted ρ vs. $1/q_L$ as irradiance increased from 0 to saturating levels. We again found that a single phase exponential decay described the relation between ρ versus $1/q$ for *Thalassiosira* from both growth light levels, although the statistical significance of support for a single fit was borderline compared to separate fits for the two growth light levels.

ρ and q_L decreased to minimal levels under the saturating light treatment but only q_L completely recovered within the first 10 s of dark recovery period (Fig. 15A and B). YNPQ was induced to a higher maximum for *Thalassiosira* from saturating growth light (Fig. 15C). For cultures from growth limiting light σ_{PSII} increased under the light treatment and gradually decreased to the initial value under dark conditions. For cultures from growth saturating light σ_{PSII} decreased under light treatment and recovered to the initial value after the first 10 s of dark recovery, in a mirror image of the pattern of YNPQ (compare Fig. 15D with Fig. 15C).

4. Discussion

4.1. Effect of FRR settings and initial ρ across taxa

The setting of FRR flashlet intensity [34,35] affected the value of ρ from fits of fluorescence induction curves in all the studied species, where high flashlet intensity led to under-estimated ρ , while low flashlet intensity led to over-estimated ρ . A previous study found in contrast that a lower flashlet intensity which did not saturate fluorescence in *Chlorella pyrenoidosa* under-estimated ρ [5]. Using a protocol to set optimum flashlet intensity we found that the initial values of ρ ranged from a low of 0.18 in *Synechococcus* to 0.43 in *Ostreococcus*, consistent with $0 < \rho < 0.5$ in previous studies [5,12,13,45], showing that ρ can vary widely among species.

4.2. Effects of increasing light on ρ' , q_L , and σ_{PSII}'

Understanding the relations among ρ' and σ_{PSII}' in the four phytoplankton species could help us understand the fates of energy absorbed by light harvesting antenna and PSII response mechanisms under varied light conditions. When Joliot and Joliot [7] proposed the notion of ρ , they concluded that an exciton that visits a closed PSII RC can be redirected to an open PSII RC, so that the trapping cross section of remaining open PSII RC increases as their neighbors become closed. Therefore σ_{PSII}' of remaining open PSII RC should increase when neighbors become closed by actinic light. In this study, we observed that σ_{PSII}' significantly increased in *Synechococcus* first transferred from dark to low actinic light intensity from the dark (Fig. 6G) likely reflecting a state 2 to state 1 transition [18,41], but that σ_{PSII}' did not then change when actinic light continued to increase and PSII RC progressively closed. Moreover, we did not see any progressive increase of σ_{PSII}' when PSII RC progressively closed under actinic light in the other three taxa studied, contrary to the model of Joliot and Joliot [7] that σ_{PSII}' of PSII RC will increase as neighboring PSII RC are closed. Our results rather show that across four structurally diverse taxa ρ' drops quickly under actinic light and therefore the remaining exciton transfer among PSII is not strong enough to measurably affect the σ_{PSII}' in remaining open PSII RC, a precedent found in *Chlorella vulgaris* [9].

As actinic light increased to saturating levels in all species, ρ' decreased to minimal levels. In some cases estimated ρ' then re-increased with further increases in actinic light. The remaining variable fluorescence was however too small to accurately fit the values of ρ' under high light in *Prochlorococcus*, *Synechococcus* and *Ostreococcus*. Furthermore, ρ' 1 s measured after 1 s of darkness remained low after exposure to super-saturating light. We are therefore not confident in the increasing fitted ρ' values measured under super-saturating light in *Prochlorococcus*, *Synechococcus* and *Ostreococcus*. ρ' remained low even under super-saturating light in *Thalassiosira* (Fig. 6A). We therefore suspect that actual ρ' is minimal under super-saturating light to pre-

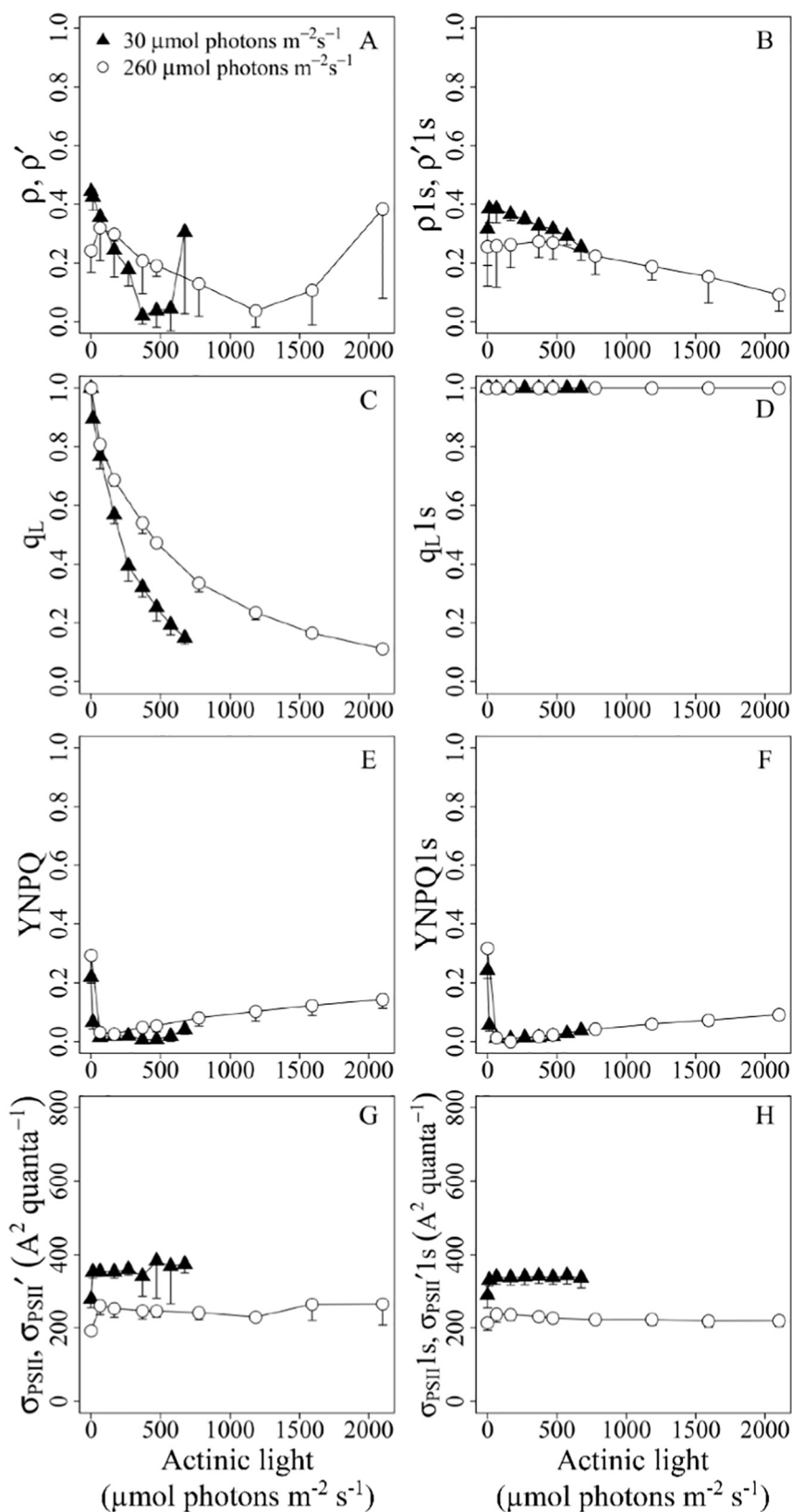


Fig. 6. Responses of Photosystem II to increasing light intensity in *Synechococcus*. Cultures from growth limiting (filled triangles) or growth saturating light (empty circles); $n = 4-8$ independently grown cultures, means \pm S.D. (A) Coefficient of excitation transfer among PSII units under actinic light (ρ) or (B) after 1 s dark following actinic light ($\rho'1s$). (C) Coefficient of photochemical quenching under actinic light (q_L) or (D) after 1 s dark following actinic light (q_L1s). (E) Yield of non-photochemical quenching under actinic light (YNPQ) or (F) after 1 s dark following actinic light (YNPQ1s). (G) Effective absorption cross section for PSII photochemistry under actinic light (σ_{PSII}) ($\text{A}^2 \text{ quanta}^{-1}$) or (H) after 1 s dark following actinic light ($\sigma_{\text{PSII}}1s$).

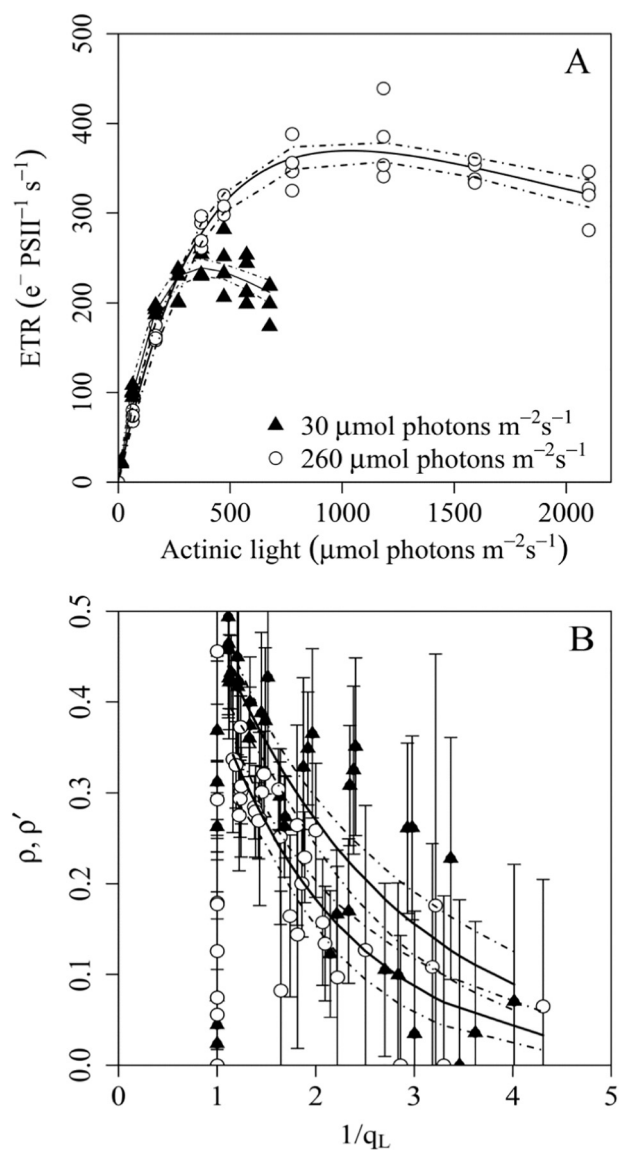
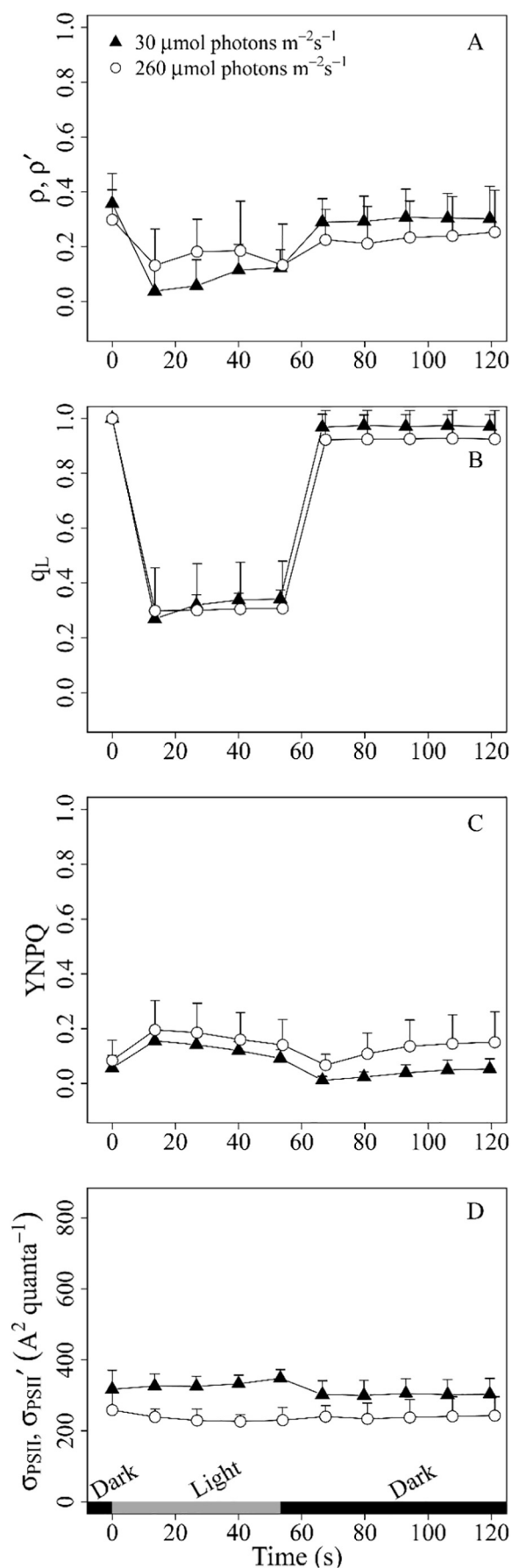


Fig. 7. Light response curves of *Synechococcus*. (A) Electron transport rate (ETR) response to increasing light. Cultures from growth limiting (filled triangles) or growth saturating light (empty circles) were fit with the equation from Fig. 4A. Dotted lines show 95% confidence interval of regression lines. Fitting data from the two growth lights separately gave a significantly better fit than a common fit of all data pooled ($F = 153.5$, $P < 0.05$). $n = 4$ independently grown cultures, means \pm S.D. (B) Coefficient of excitation transfer among PSII units (ρ, ρ') plotted against the reciprocal of simultaneously determined coefficient of photochemical quenching ($1/q_L$). Cultures were exposed to 0 to $527 \mu\text{mol photons m}^{-2} \text{s}^{-1}$ (filled triangles) or 0 to $1185 \mu\text{mol photons m}^{-2} \text{s}^{-1}$ (open circles). Error bars on ρ determinations show the 95% confidence interval on the fitted parameter from an individual measurement. Nonlinear regression lines were fit to the data pooled from $30 \mu\text{mol photons m}^{-2} \text{s}^{-1}$ ($r^2 = 0.75$, Summed square of residuals = 0.17, Residual standard error = 0.23, Exponential decay rate = 0.55) or $260 \mu\text{mol photons m}^{-2} \text{s}^{-1}$ ($r^2 = 0.72$, Summed square of residuals = 0.09, Residual standard error = 0.18) according to the same equation as Fig. 4B. Below dotted lines show 95% confidence interval of the regression lines. Fitting data from the two growth lights separately gave a significantly better fit than a common fit of all data pooled ($F = 19.82$, $P < 0.05$). $n = 4$ independently grown cultures, means \pm S.D.

empt dangerous increases in $\sigma_{\text{PSII}'}$ [46] in these phytoplankton.

A simple approximation of an evenly spaced two dimensional matrix of PSII RC shows that distance among remaining open PSII RC is a linear function of the reciprocal of the fraction of remaining open PSII RC, $1/q_L$. Our results support previous work that excitonic connectivity among PSII declines rapidly beyond a certain distance among open PSII [47]. Furthermore the decay of ρ versus $1/q_L$ suggests an accessible approach to rapidly analyze the comparative spacing of



(caption on next page)

Fig. 8. Changes in Photosystem II function under initial darkness, saturating actinic light and subsequent dark recovery in *Synechococcus*. Cultures were measured in darkness (0 s), exposed to saturating light and shifted back to darkness. $n = 4$ independently grown cultures, means \pm S.D. (A) Excitation transfer among PSII units (ρ). (B) Coefficient of photochemical quenching (q_L). (C) Yield of non-photochemical quenching (YNPQ). (D) The effective absorption cross section for PSII (σ_{PSII} or σ_{PSII}' ; $A^2 \text{ quanta}^{-1}$).

PSII centres across taxa with diverse thylakoid architectures. We were able to fit an exponential decay correlating ρ with $1/q$, but the curve fits differed among the taxa, showing differential responses of ρ to progressive PSII closure among the taxa. To drive ρ down to the minimal level of 0.1 required a q_L of 0.26 in *Synechococcus* from growth limiting light; 0.3 in *Thalassiosira*; 0.35 in *Synechococcus* from growth saturating light; 0.42 in *Prochlorococcus*; and 0.5 in *Ostreococcus*. This suggests the effective distance among PSII RC [48,49] is greatest in the chl a/b prasinophyte green algae *Ostreococcus* compared to the other taxa because less PSII closure is required to reach minimal ρ in *Ostreococcus*. Indeed, measured distances between PSII RC vary from 12.8 nm in the cyanobacteria *Synechocystis*, up to 24 nm in grana thylakoids of spinach (*Spinacea oleraceae* var. polka) [49,50]. For *Synechococcus* we found significantly lower initial ρ for cultures from growth saturating light compared to cultures from growth limiting light [51]. Interestingly *Synechococcus* was also the only of our test taxa that showed a statistically distinct relation between ρ and $1/q_L$ depending upon growth light. We long ago found that in another strain of *Synechococcus* the low light isoform of PsbA protein supported larger state transitions and concomitant changes in excitation distribution compared to the high light isoform. We now suspect that the distinct patterns of ρ versus PSII closure in *Synechococcus* WH8102 also reflect different isoform compositions of PsbA depending upon growth light. Alternately, or in parallel, *Synechococcus* may increase the spacing distance between PSII centers with increasing growth light, to a greater extent than found in the other tested taxa.

4.3. Effect of saturating light and subsequent recovery upon ρ and NPQ

In *Prochlorococcus* ρ recovered in direct parallel with the reopening of PSII RC in darkness after exposure to saturating light. In contrast in *Synechococcus* after a saturating light treatment ρ recovered faster under low actinic light compared to darkness (Fig. 9). Respiration can affect the redox state of the PQ pool, leading to a transition from state 1 to state 2 in darkness in cyanobacteria [41]. In our study, *Synechococcus* transitioned from state 1 to state 2 under dark recovery but remained in state 1 under low light recovery. We suggest that in *Synechococcus* under state 1 increased connectivity among PSII helps ρ to completely recover to the initial low light ρ' value, compared to a slower recovery of ρ under state 2 in darkness [44,52] when excitation flow from PSII to PSI, and/or from phycobilisomes to PSI, competes with PSII-PSII excitonic connectivity.

Following the saturating light treatment in *Ostreococcus* ρ did not completely recover to initial values even when q_L completely recovered within the first 10 s dark. In *Ostreococcus* the delay in recovery of ρ was paralleled by an incomplete recovery of σ_{PSII}' within the first 10 s of dark. We suggest that a sustained form of NPQ competes for excitation [53] thereby, down-regulating both ρ and σ_{PSII}' . Indeed ρ was also lower in shade leaves compared to sun exposed leaves of *Hordeum vulgare* L. [54], a pattern correlated with excitation dissipation in that species. In *Thalassiosira*, as in *Ostreococcus*, ρ did not completely recover to initial values even though q_L completely recovered within the first 1 s of dark. However, contrary to *Ostreococcus*, in *Thalassiosira* σ_{PSII} did not completely recover within the first 10 s of dark. These results suggest another physiological mechanism in diatoms, beyond the proportion of remaining open PSII RC (q_L) and connectivity mediated by σ_{PSII} , which delays ρ recovery within the first 10 s of dark. Membrane and PSII particle spacing can change within minutes in spinach chloroplasts [55,56] so spacing of PSII might also be changed by illumination in

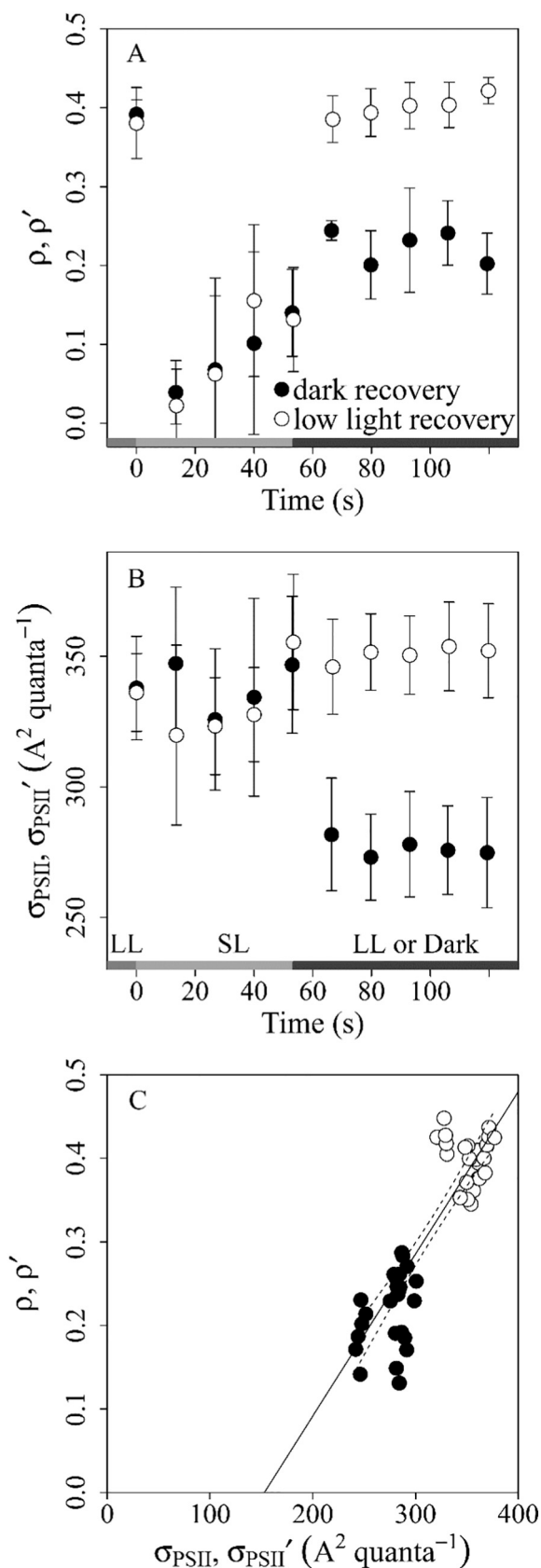


Fig. 9. The effect of state transitions on PSII function under actinic light treatment and dark recovery in *Synechococcus*. (A) Excitation transfer among PSII units (ρ and ρ') (B) The effective absorption cross section for PSII (σ_{PSII} and σ_{PSII}'). (C) ρ and ρ' plotted against σ_{PSII} and σ_{PSII}' during the dark recovery period. The black solid line shows a regression line fit to the data while the black dotted line shows the 95% confidence interval of regression; $y = 0.0019 * x - 0.2968$, R -squared = 0.79. $n = 4$ independently grown cultures, means \pm S.D.

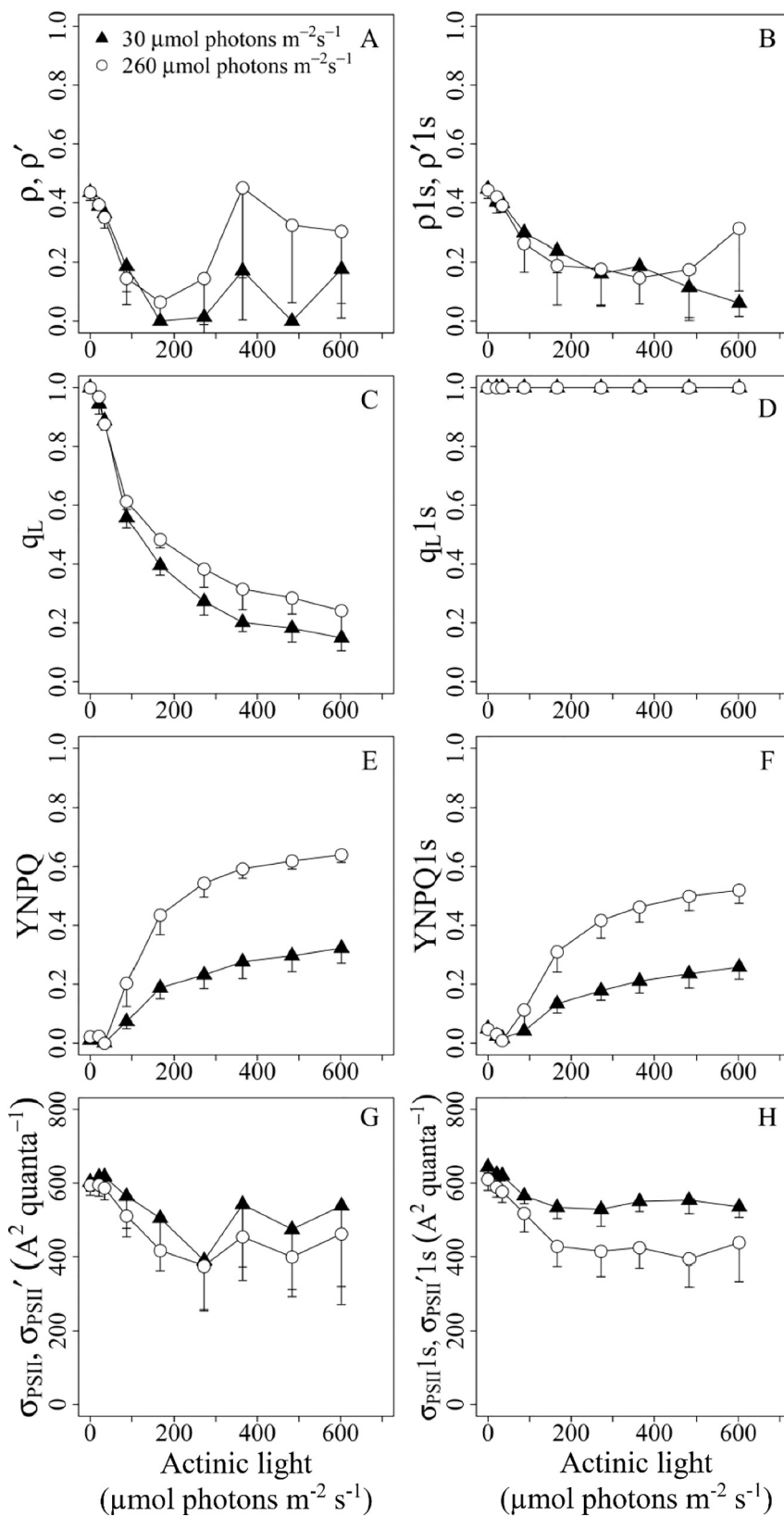


Fig. 10. Responses of Photosystem II to increasing light intensity in *Ostreococcus*. Cultures from growth limiting (filled triangles) or growth saturating light (empty circles); $n = 5$ independently grown cultures, means \pm S.D. (A) Coefficient of excitation transfer among PSII units under actinic light (ρ') or (B) after 1 s dark following actinic light ($\rho'1s$). (C) Coefficient of photochemical quenching under actinic light (q_L) or (D) after 1 s dark following actinic light (q_L1s); (E) Yield of non-photochemical quenching under actinic light (YNPQ) or (F) after 1 s dark following actinic light (YNPQ1s). (G) Effective absorption cross section for PSII photochemistry under actinic light (σ_{PSII}) ($A^2 \text{ quanta}^{-1}$) or (H) after 1 s dark following actinic light ($\sigma_{PSII}1s$).

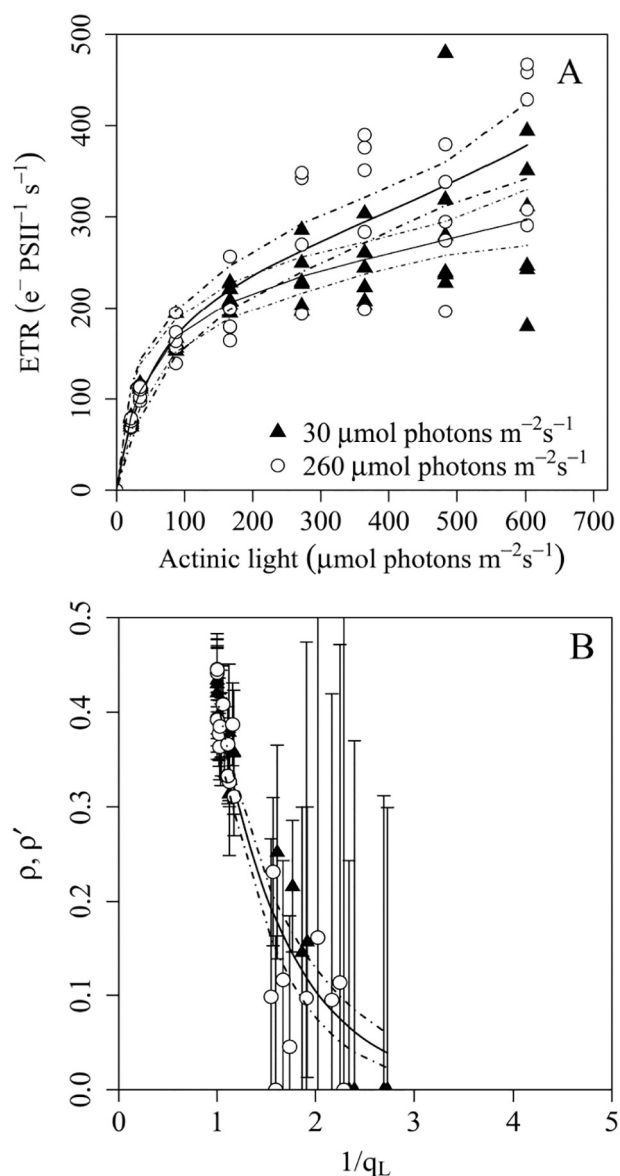


Fig. 11. Light response curves of *Ostreococcus*. (A) Electron transport rate (ETR) response to increasing light. Cultures from growth limiting (filled triangles) or growth saturating light (empty circles) were fit with the equation from Fig. 4A. Dotted lines show 95% confidence interval of regression line. Fitting data from the two growth lights separately give a significantly better fit than a common fit of all data pooled ($F = 6.06$, $P < 0.05$). $n = 5$ independently grown cultures, means \pm S.D. (B) Coefficient of excitation transfer among PSII units (ρ, ρ') plotted against the reciprocal of simultaneously determined coefficient of photochemical quenching ($1/q_L$). Cultures were exposed to 0 to 167 $\mu\text{mol photons m}^{-2}\text{s}^{-1}$ (filled triangles) or to 0 to 206 $\mu\text{mol photons m}^{-2}\text{s}^{-1}$ (empty circles). Error bars on ρ determinations show the 95% confidence interval on the fitted parameter from an individual measurement. A nonlinear regression line (as in Fig. 4B) was fit to the data pooled from both growth lights ($r^2 = 0.87$, Summed square of residuals = 0.10, Residual standard error = 0.15, Exponential decay rate = 1.35). Black dotted lines show 95% confidence interval of the regression line. Fitting data from the two growth lights separately did not show a significantly better fit than a common fit of all data pooled ($F = 2.44$, $P > 0.05$). $n = 5$ independently grown cultures, means \pm S.D.

eukaryotic diatoms. Re-establishing the spacing among PSII under darkness could delay ρ recovery in diatoms.

5. Conclusion

When PSII RC closed under increasing actinic light $\sigma_{\text{PSII}'}$ did not increase, because ρ decreased from initial levels. This decrease in ρ is largely explicable in terms of an increase in the distance among

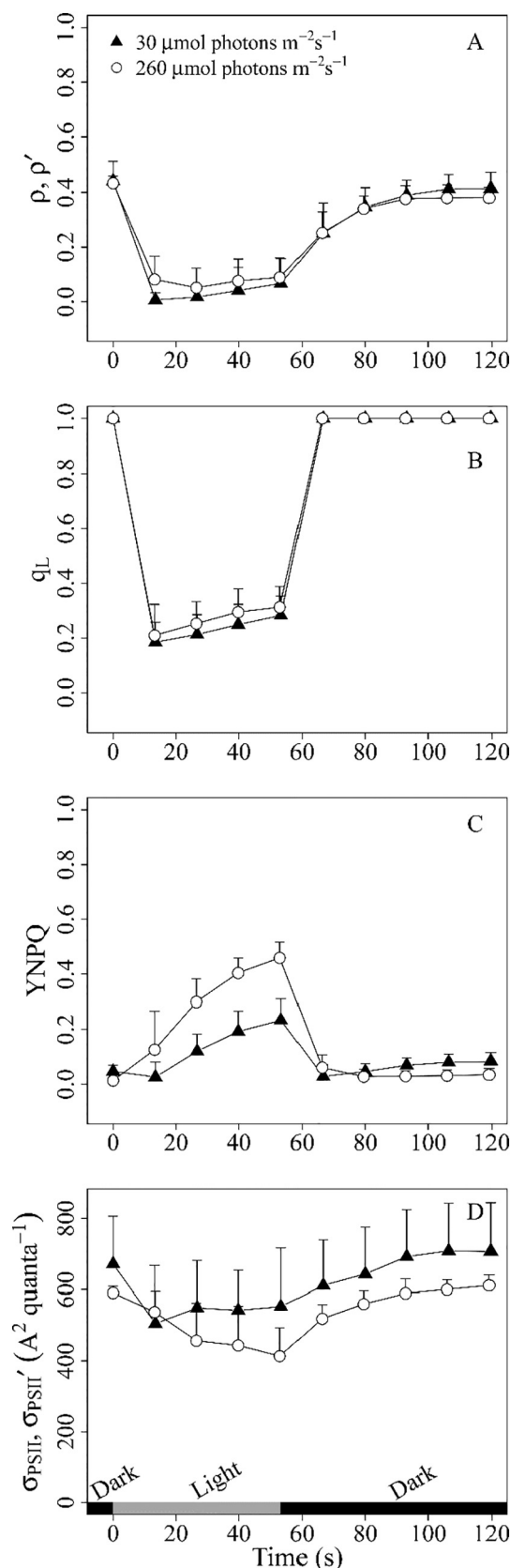


Fig. 12. Changes in Photosystem II function under initial darkness, saturating actinic light and subsequent dark recovery in *Ostreococcus*. Cultures were measured in darkness (0 s), then exposed to saturating light and shifted back to darkness. $n = 5$ independently grown cultures, means \pm S.D. (A) Excitation transfer among PSII units (ρ). (B) Coefficient of photochemical quenching (q_L). (C) Yield of non-photochemical quenching (YNPQ). (D) The effective absorption cross section for PSII (σ_{PSII} or $\sigma_{\text{PSII}'}$; $\text{A}^2 \text{ quanta}^{-1}$).

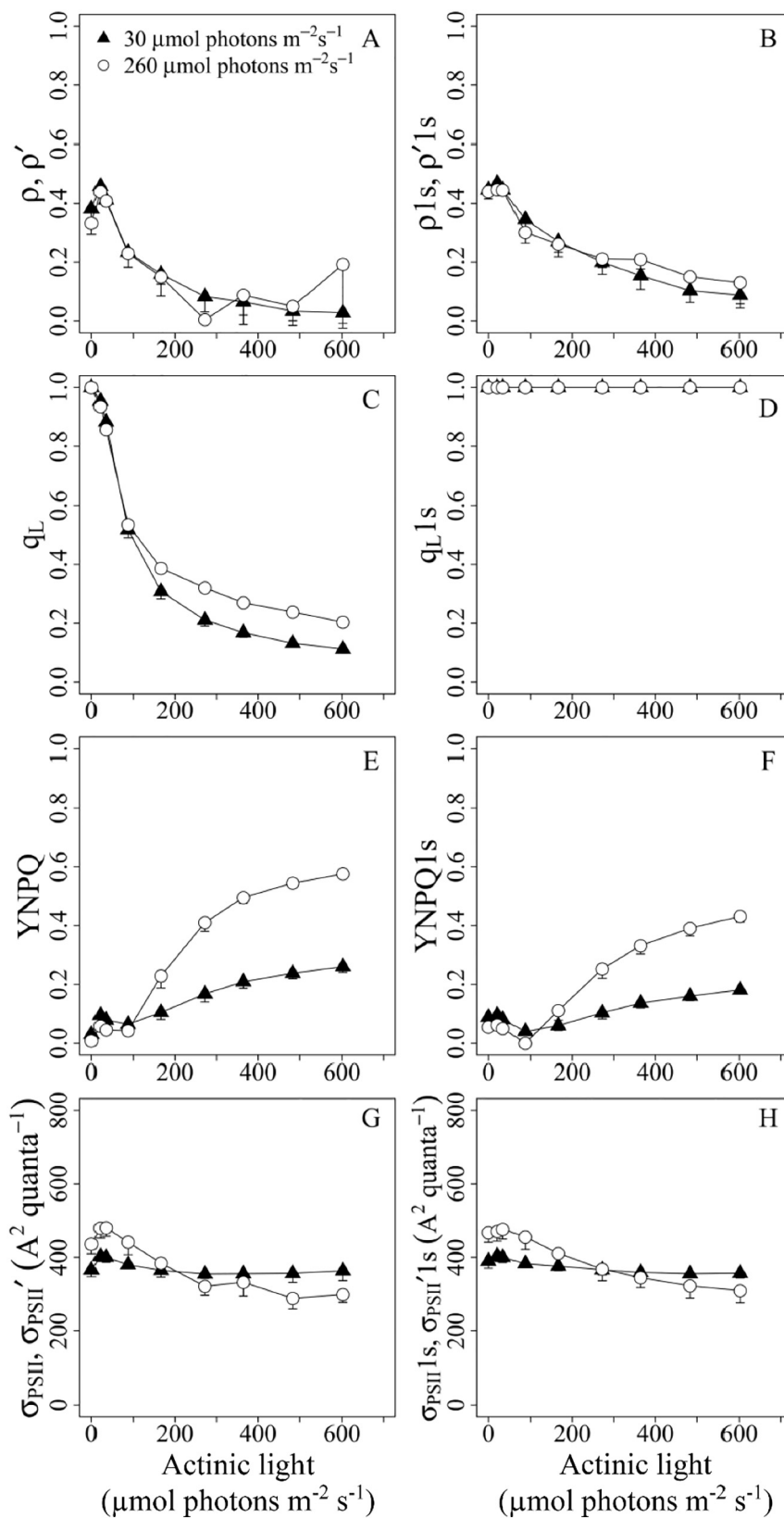


Fig. 13. Responses of Photosystem II to increasing light intensity in *Thalassiosira*. Cultures from growth limiting (filled triangles) or growth saturating light (empty circles); $n = 4-6$ independently grown cultures, means \pm S.D. (A) Coefficient of excitation transfer among PSII units under actinic light (ρ) or (B) after 1 s dark ($\rho'1s$). (C) Coefficient of photochemical quenching under actinic light (q_L) or (D) after 1 s dark following actinic light (q_L1s). (E) Yield of non-photochemical quenching under actinic light (YNPQ) or (F) after 1 s dark following actinic light (YNPQ1s). (G) Effective absorption cross section for PSII photochemistry under actinic light ($A^2 \text{ quanta}^{-1}$, σ_{PSII} under $0 \mu\text{mol photons m}^{-2} \text{ s}^{-1}$, σ_{PSII}' under illumination) or (H) after 1 s dark following initial dark ($\sigma_{PSII}1s$) and actinic light ($\sigma_{PSII}'1s$).

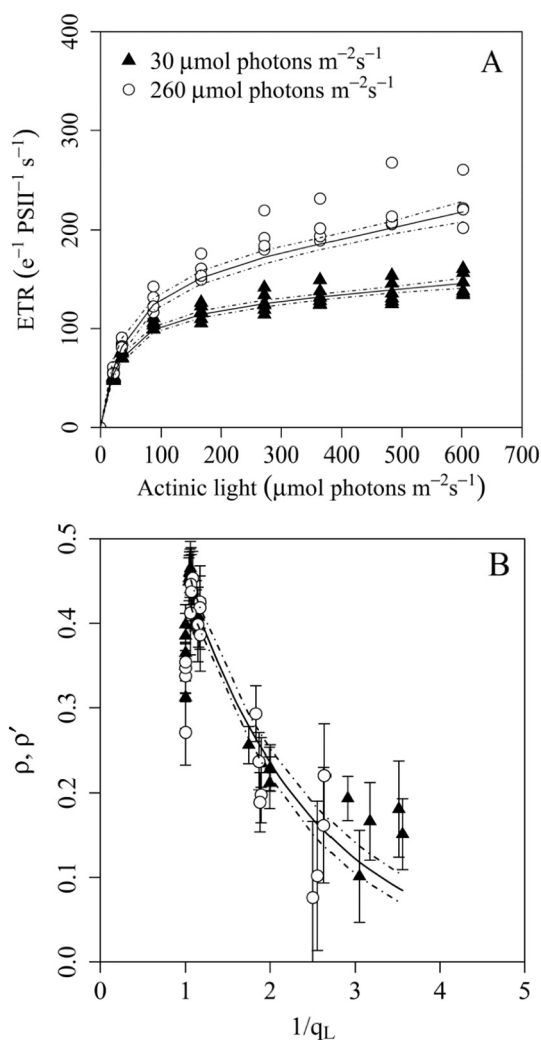


Fig. 14. Light response curves of *Thalassiosira*. (A) Electron transport rate (ETR) response to increasing light. Cultures from growth limiting (filled triangles) or growth saturating light (empty circles) were fit with the equation from Fig. 4A. Dotted lines show 95% confidence interval of the regression lines. Fitting data from the two growth lights separately gave a significantly better fit than a common fit of all data pooled ($F = 17.0$, $P < 0.05$). $n = 4-6$ independently grown cultures, means \pm S.D. (B) Coefficient of excitation transfer among PSII units (ρ, ρ') plotted against the reciprocal of simultaneously determined coefficient of photochemical quenching ($1/q_L$). Cultures were exposed to 0 to 272 $\mu\text{mol photons m}^{-2}\text{s}^{-1}$ (filled triangles) or 0 to 272 $\mu\text{mol photons m}^{-2}\text{s}^{-1}$ (empty circles). Error bars on ρ determinations show the 95% confidence interval on the fitted parameter from an individual measurement. A nonlinear regression line was fit to the data pooled from both growth lights ($r^2 = 0.91$, Summed square of residuals = 0.05, Residual standard error = 0.19, Exponential decay rate = 0.66) according to the equation Fig. 4B. Black dotted lines show 95% confidence interval of the regression line. Fitting data from the two growth lights separately did not show a significantly better fit than a common fit of all data pooled ($F = 2.0$, $P > 0.05$). $n = 4-6$ independently grown cultures, means \pm S.D.

remaining open PSII RC with increasing actinic light, although the responsiveness of ρ to PSII closure varied across taxa, likely reflecting differences in spacing among PSII. Subsequent to the initial down regulation ρ , recovery under darkness or low light is directly attributable to PSII re-opening in *Prochlorococcus*. In the other taxa even after PSII has re-opened three distinct mechanisms intervene to delay the recovery of ρ . We suggest that the patterns versus PSII closure ρ' can provide a convenient means to compare differences in PSII spacing across structurally diverse taxa.

Supplementary data to this article can be found online at <http://dx.doi.org/10.1016/j.bbabo.2017.03.003>.

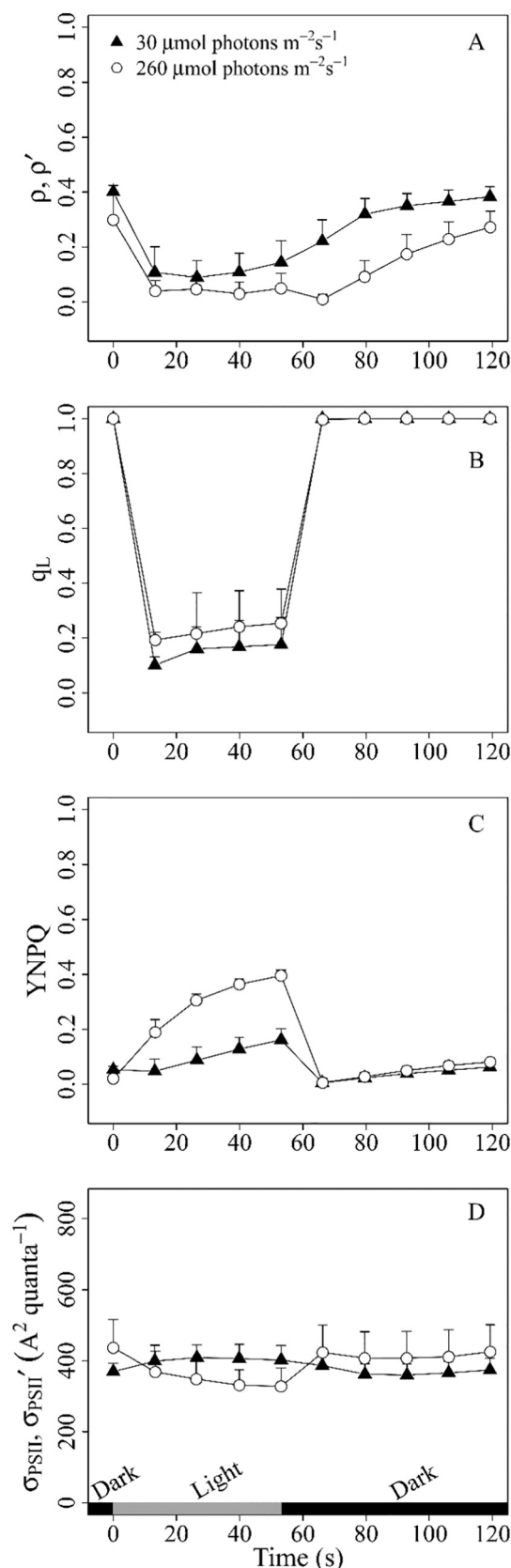


Fig. 15. Changes in Photosystem II function under initial darkness, saturating actinic light and subsequent dark recovery in *Thalassiosira*. Cultures were measured in darkness (0 s), exposed to saturating light and shifted back to darkness. $n = 4-6$ independently grown cultures, means \pm S.D. (A) Excitation transfer among PSII units (ρ). (B) Coefficient of photochemical quenching (q_L). (C) Yield of non-photochemical quenching (YNPQ). (D) The effective absorption cross section for PSII (σ_{PSII} or σ_{PSII}' ; $\text{A}^2 \text{ quanta}^{-1}$).

Transparency Document

The <http://dx.doi.org/10.1016/j.bbabi.2017.03.003> associated with this article can be found in the online version.

Acknowledgements

This study was funded by the Natural Sciences and Engineering Research Council of Canada (DC, JGB) and the Canada Research Chairs (DC) using equipment funded by the New Brunswick Innovation Foundation (DC) and the Canada Foundation for Innovation (DC). The authors thank M. Gorbunov for helpful discussions.

References

- [1] A. Stirbet, Excitonic connectivity between photosystem II units: what is it, and how to measure it? *Photosynth. Res.* 116 (2013) 189–214, <http://dx.doi.org/10.1007/s11120-013-9863-9>.
- [2] F. Cho, Govindjee, Low-temperature (4–77 K) spectroscopy of chloroella; temperature dependence of energy transfer efficiency, *Biochim. Biophys. Acta BBA - Bioenergy* 216 (1970) 139–150, [http://dx.doi.org/10.1016/0005-2728\(70\)90166-0](http://dx.doi.org/10.1016/0005-2728(70)90166-0).
- [3] H. van Amerongen, R. van Grondelle, Understanding the energy transfer function of LHCII, the major light-harvesting complex of green plants, *J. Phys. Chem. B* 105 (2001) 604–617, <http://dx.doi.org/10.1021/jp0028406>.
- [4] W.L. Butler, Energy transfer between photosystem II units in a connected package model of the photochemical apparatus of photosynthesis, *Proc. Natl. Acad. Sci. U. S. A.* 77 (1980) 4697–4701.
- [5] Z.S. Kolber, O. Prášil, P.G. Falkowski, Measurements of variable chlorophyll fluorescence using fast repetition rate techniques: defining methodology and experimental protocols, *Biochim. Biophys. Acta BBA - Bioenergy* 1367 (1998) 88–106, [http://dx.doi.org/10.1016/S0005-2728\(98\)00135-2](http://dx.doi.org/10.1016/S0005-2728(98)00135-2).
- [6] P. Joliot, P. Bennoun, A. Joliot, New evidence supporting energy transfer between photosynthetic units, *Biochim. Biophys. Acta BBA - Bioenergy* 305 (1973) 317–328, [http://dx.doi.org/10.1016/0005-2728\(73\)90179-5](http://dx.doi.org/10.1016/0005-2728(73)90179-5).
- [7] A. Joliot, P. Joliot, Étude cinétique de la réaction photochimique libérant l'oxygène au cours de la photosynthèse, *CR Acad. Sci. Paris* 258 (1964) 4622–4625.
- [8] D.C. Mauzerall, Evidence that the variable fluorescence in *Chlorella* is recombination luminescence, *Biochim. Biophys. Acta* 809 (1985) 11–16.
- [9] A.C. Ley, D.C. Mauzerall, The extent of energy transfer among Photosystem II reaction centers in *Chlorella*, *Biochim. Biophys. Acta BBA - Bioenergy* 850 (1986) 234–248, [http://dx.doi.org/10.1016/0005-2728\(86\)90178-7](http://dx.doi.org/10.1016/0005-2728(86)90178-7).
- [10] D.J. Suggett, H.L. MacIntyre, T.M. Kana, R.J. Geider, Comparing electron transport with gas exchange: parameterising exchange rates between alternative photosynthetic currencies for eukaryotic phytoplankton, *Res. Gate* 56 (2009) 147–162, <http://dx.doi.org/10.3354/ame01303>.
- [11] M.J. Behrenfeld, Z.S. Kolber, Widespread iron limitation of phytoplankton in the south pacific ocean, *Science* 283 (1999) 840–843.
- [12] S.W. Liu, B.S. Qiu, Different responses of photosynthesis and flow cytometric signals to iron limitation and nitrogen source in coastal and oceanic *Synechococcus* strains (Cyanophyceae), *Mar. Biol.* 159 (2012) 519–532, <http://dx.doi.org/10.1007/s00227-011-1832-2>.
- [13] S. Trimborn, S. Thoms, K. Petrou, S.A. Kranz, B. Rost, Photophysiological responses of Southern Ocean phytoplankton to changes in CO₂ concentrations: short-term versus acclimation effects, *J. Exp. Mar. Biol. Ecol.* 451 (2014) 44–54, <http://dx.doi.org/10.1016/j.jembe.2013.11.001>.
- [14] J.B. Sylvan, A. Quigg, S. Tozzi, J.W. Ammerman, Eutrophication-induced phosphorus limitation in the Mississippi River plume: evidence from fast repetition rate fluorometry, *Limnol. Oceanogr.* 52 (2007) 2679–2685, <http://dx.doi.org/10.4319/lo.2007.52.6.2679>.
- [15] D.J. Suggett, C.M. Moore, A. Hickman, R.J. Geider, Interpretation of fast repetition rate (FRR) fluorescence: signatures of phytoplankton community structure versus physiological state, *Mar. Ecol. Prog. Ser.* 376 (2009) 1–19, <http://dx.doi.org/10.3354/meps07830>.
- [16] D.J. Suggett, H.L. MacIntyre, R.J. Geider, Evaluation of biophysical and optical determinations of light absorption by photosystem II in phytoplankton, *Limnol. Oceanogr. Methods* 2 (2004) 316–332, <http://dx.doi.org/10.4319/lom.2004.2.316>.
- [17] M. Olaiola, J. La Roche, Z. Kolber, P.G. Falkowski, Non-photochemical fluorescence quenching and the diadinoxanthin cycle in a marine diatom, *Photosynth. Res.* 41 (1994) 357–370, <http://dx.doi.org/10.1007/BF00019413>.
- [18] M.D. McConnell, R. Koop, S. Vasil'ev, D. Bruce, Regulation of the distribution of chlorophyll and phycobilin-absorbed excitation energy in Cyanobacteria. A structure-based model for the light state transition, *Plant Physiol.* 130 (2002) 1201–1212, <http://dx.doi.org/10.1104/pp.009845>.
- [19] M. Ragni, R.L. Airs, N. Leonardos, R.J. Geider, Photoinhibition of PSII in *Emiliania huxleyi* (haptophyta) under high light stress: the roles of photoacclimation, photoprotection, and photorepair, *J. Phycol.* 44 (2008) 670–683, <http://dx.doi.org/10.1111/j.1529-8817.2008.00524.x>.
- [20] P.G. Falkowski, T.G. Owens, Light—shade adaptation 1, *Plant Physiol.* 66 (1980) 592–595.
- [21] Y. Huot, M. Babin, Overview of fluorescence protocols: theory, basic concepts, and practice, in: D.J. Suggett, O. Prášil, M.A. Borowitzka (Eds.), *Chlorophyll Fluoresc.*, *Aquat. Sci. Methods Appl.*, Springer, Netherlands, 2010, pp. 31–74 (http://link.springer.com/chapter/10.1007/978-90-481-9268-7_3 accessed June 10, 2014).
- [22] E. Lawrenz, G. Silsbe, E. Capuzzo, P. Ylöstalo, R.M. Forster, S.G.H. Simis, O. Prášil, J.C. Kromkamp, A.E. Hickman, C.M. Moore, M.-H. Forget, R.J. Geider, D.J. Suggett, Predicting the electron requirement for carbon fixation in seas and oceans, *PLoS One* 8 (2013) e58137, <http://dx.doi.org/10.1371/journal.pone.0058137>.
- [23] G.M. Silsbe, K. Oxborough, D.J. Suggett, R.M. Forster, S. Ihnken, O. Komárek, E. Lawrenz, O. Prášil, R. Röttgers, M. Šicner, S.G.H. Simis, M.A. Van Dijk, J.C. Kromkamp, Toward autonomous measurements of photosynthetic electron transport rates: an evaluation of active fluorescence-based measurements of photochemistry, *Limnol. Oceanogr. Methods* 13 (2015) 138–155, <http://dx.doi.org/10.1002/lom3.10014>.
- [24] K. Oxborough, C.M. Moore, D.J. Suggett, T. Lawson, H.G. Chan, R.J. Geider, Direct estimation of functional PSII reaction center concentration and PSII electron flux on a volume basis: a new approach to the analysis of Fast Repetition Rate fluorometry (FRRF) data, *Limnol. Oceanogr. Methods* 10 (2012) 142–154, <http://dx.doi.org/10.4319/lom.2012.10.142>.
- [25] C.D. Murphy, G. Ni, G. Li, A. Barnett, K. Xu, J. Grant-Burt, J.D. Liefer, D.J. Suggett, D.A. Campbell, Quantitating active photosystem II reaction center content from fluorescence induction transients, *Limnol. Oceanogr. Methods* (2016). <http://dx.doi.org/10.1002/lom3.10142> (n/a–n/a).
- [26] A. Morel, Y.-H. Ahn, F. Partensky, D. Vault, H. Claustre, *Prochlorococcus* and *Synechococcus*: a comparative study of their optical properties in relation to their size and pigmentation, *J. Mar. Res.* 51 (1993) 617–649, <http://dx.doi.org/10.1357/0022240933223963>.
- [27] G. Rocap, F.W. Larimer, J. Lamerdin, S. Malfatti, P. Chain, N.A. Ahlgren, A. Arellano, M. Coleman, L. Hauser, W.R. Hess, Z.I. Johnson, M. Land, D. Lindell, A.F. Post, W. Regala, M. Shah, S.L. Shaw, C. Steglich, M.B. Sullivan, C.S. Ting, A. Tolonen, E.A. Webb, E.R. Zinser, S.W. Chisholm, Genome divergence in two *Prochlorococcus* ecotypes reflects oceanic niche differentiation, *Nature* 424 (2003) 1042–1047, <http://dx.doi.org/10.1038/nature01947>.
- [28] D. Li, J. Xie, J. Zhao, A. Xia, D. Li, Y. Gong, Light-induced excitation energy redistribution in *Spirulina platensis* cells: “spillover” or “mobile PBSs”? *Biochim. Biophys. Acta BBA - Bioenergy* 1608 (2004) 114–121, <http://dx.doi.org/10.1016/j.bbabi.2003.11.002>.
- [29] W.D. Swingley, M. Iwai, Y. Chen, S. Ozawa, K. Takizawa, Y. Takahashi, J. Minagawa, Characterization of photosystem I antenna proteins in the prasinophyte *Ostreococcus tauri*, *Biochim. Biophys. Acta BBA - Bioenergy* 1797 (2010) 1458–1464, <http://dx.doi.org/10.1016/j.bbabi.2010.04.017>.
- [30] T.G. Owens, Light-harvesting function in the diatom *Phaeodactylum tricornutum*: II. Distribution of excitation energy between the photosystems, *Plant Physiol.* 80 (1986) 739–746.
- [31] L.R. Moore, A. Coe, E.R. Zinser, M.A. Saito, M.B. Sullivan, D. Lindell, K. Frois-Moniz, J. Waterbury, S.W. Chisholm, Culturing the marine cyanobacterium *Prochlorococcus*, *Limnol. Oceanogr. Methods* 5 (2007) 353–362, <http://dx.doi.org/10.4319/lom.2007.5.353>.
- [32] R.R.L. Guillard, P.E. Hargraves, *Stichochrysis immobilis* is a diatom, not a chryso-phyte, *Phycologia* 32 (1993) 234–236, <http://dx.doi.org/10.2216/i0031-8884-32-3-234.1>.
- [33] R.R.L. Guillard, J.H. Ryther, Studies of marine planktonic diatoms: I. *Cyclotella nana* Husted, and *Detonula confervacea* (Cleve) Gran, *Can. J. Microbiol.* 8 (1962) 229–239, <http://dx.doi.org/10.1139/m62-029>.
- [34] S.R. Laney, Assessing the error in photosynthetic properties determined with Fast Repetition Rate fluorometry, *Limnol. Oceanogr.* 48 (2003) 2234–2242.
- [35] S.R. Laney, R.M. Letelier, Artifacts in measurements of chlorophyll fluorescence transients, with specific application to fast repetition rate fluorometry, *Limnol. Oceanogr. Methods* 6 (2008) 40–50, <http://dx.doi.org/10.4319/lom.2008.6.40>.
- [36] G. Ni, G. Zimbalatti, C.D. Murphy, A.B. Barnett, C.M. Arsenault, G. Li, A.M. Cockshutt, D.A. Campbell, Arctic *Micromonas* uses protein pools and non-photochemical quenching to cope with temperature restrictions on Photosystem II protein turnover, *Photosynth. Res.* (2016). <http://dx.doi.org/10.1007/s11120-016-0310-6>.
- [37] K. Oxborough, N.R. Baker, Resolving chlorophyll *a* fluorescence images of photosynthetic efficiency into photochemical and non-photochemical components – calculation of qP and Fv'/Fm'; without measuring F_o', *Photosynth. Res.* 54 (1997) 135–142, <http://dx.doi.org/10.1023/A:1005936823310>.
- [38] D.M. Kramer, G. Johnson, O. Kiirats, G.E. Edwards, New fluorescence parameters for the determination of Q_A redox state and excitation energy fluxes, *Photosynth. Res.* 79 (2004) 209–218, <http://dx.doi.org/10.1023/B:PRES.0000015391.99477.0d>.
- [39] C. Klughammer, U. Schreiber, Complementary PS II quantum yields calculated from simple fluorescence parameters measured by PAM fluorometry and the Saturation Pulse method, *PAM Appl. Notes* 1 (2008) 27–35.
- [40] J. Serôdio, S. Cruz, S. Vieira, V. Brotas, Non-photochemical quenching of chlorophyll fluorescence and operation of the xanthophyll cycle in estuarine microphytobenthos, *J. Exp. Mar. Biol. Ecol.* 326 (2005) 157–169, <http://dx.doi.org/10.1016/j.jembe.2005.05.011>.
- [41] D. Campbell, V. Hurry, A.K. Clarke, P. Gustafsson, G. Öquist, Chlorophyll fluorescence analysis of cyanobacterial photosynthesis and acclimation, *Microbiol. Mol. Biol. Rev.* 62 (1998) 667–683.
- [42] P.H.C. Eilers, J.C.H. Peeters, A model for the relationship between light intensity and the rate of photosynthesis in phytoplankton, *Ecol. Model.* 42 (1988) 199–215, [http://dx.doi.org/10.1016/0304-3800\(88\)90057-9](http://dx.doi.org/10.1016/0304-3800(88)90057-9).
- [43] J.C.H. Peeters, P. Eilers, The relationship between light intensity and photosynthesis—a simple mathematical model, *Hydrobiol. Bull.* 12 (1978) 134–136,

- <http://dx.doi.org/10.1007/BF02260714>.
- [44] D. Kirilovsky, Modulating energy arriving at photochemical reaction centers: orange carotenoid protein-related photoprotection and state transitions, *Photosynth. Res.* 126 (2015) 3–17, <http://dx.doi.org/10.1007/s11120-014-0031-7>.
- [45] M.Y. Gorbunov, Z.S. Kolber, M.P. Lesser, P.G. Falkowski, Photosynthesis and photoprotection in symbiotic corals, *Limnol. Oceanogr.* 46 (2001) 75–85, <http://dx.doi.org/10.4319/lo.2001.46.1.0075>.
- [46] I. Vass, Role of charge recombination processes in photodamage and photoprotection of the photosystem II complex, *Physiol. Plant.* 142 (2011) 6–16, <http://dx.doi.org/10.1111/j.1399-3054.2011.01454.x>.
- [47] S. Haferkamp, W. Haase, A.A. Pascal, H. van Amerongen, H. Kirchhoff, efficient light harvesting by Photosystem II requires an optimized protein packing density in grana thylakoids, *J. Biol. Chem.* 285 (2010) 17020–17028, <http://dx.doi.org/10.1074/jbc.M109.077750>.
- [48] E.J. Boekema, J.F. van Breemen, H. van Roon, J.P. Dekker, Arrangement of photosystem II supercomplexes in crystalline macrodomains within the thylakoid membrane of green plant chloroplasts, *J. Mol. Biol.* 301 (2000) 1123–1133, <http://dx.doi.org/10.1006/jmbi.2000.4037>.
- [49] I.M. Folea, P. Zhang, E.-M. Aro, E.J. Boekema, Domain organization of photosystem II in membranes of the cyanobacterium *Synechocystis* PCC6803 investigated by electron microscopy, *FEBS Lett.* 582 (2008) 1749–1754, <http://dx.doi.org/10.1016/j.febslet.2008.04.044>.
- [50] H. Kirchhoff, I. Tremmel, W. Haase, U. Kubitscheck, Supramolecular Photosystem II Organization in Grana Thylakoid Membranes: Evidence for a Structured Arrangement[†], *Biochemistry* 43 (2004) 9204–9213, <http://dx.doi.org/10.1021/bi0494626>.
- [51] I.R. Vassiliev, Z. Kolber, K.D. Wyman, D. Mauzerall, V.K. Shukla, P.G. Falkowski, Effects of iron limitation on Photosystem II composition and light utilization in *Dunaliella tertiolecta*, *Plant Physiol.* 109 (1995) 963–972.
- [52] H. Li, D. Li, S. Yang, J. Xie, J. Zhao, The state transition mechanism—simply depending on light-on and -off in *Spirulina platensis*, *Biochim. Biophys. Acta BBA - Bioenergy* 1757 (2006) 1512–1519, <http://dx.doi.org/10.1016/j.bbabi.2006.08.009>.
- [53] C. Six, R. Sherrard, M. Lionard, S. Roy, D.A. Campbell, Photosystem II and pigment dynamics among ecotypes of the green alga *Ostreococcus*, *Plant Physiol.* 151 (2009) 379–390.
- [54] M. Zivcak, M. Brestic, H.M. Kalaji, Govindjee, Photosynthetic responses of sun- and shade-grown barley leaves to high light: is the lower PSII connectivity in shade leaves associated with protection against excess of light? *Photosynth. Res.* 119 (2014) 339–354, <http://dx.doi.org/10.1007/s11120-014-9969-8>.
- [55] M.P. Johnson, A.P. Brain, A.V. Ruban, Changes in thylakoid membrane thickness associated with the reorganization of photosystem II light harvesting complexes during photoprotective energy dissipation, *Plant Signal. Behav.* 6 (2011) 1386–1390, <http://dx.doi.org/10.4161/psb.6.9.16503>.
- [56] M.P. Johnson, T.K. Goral, C.D.P. Duffy, A.P.R. Brain, C.W. Mullineaux, A.V. Ruban, Photoprotective energy dissipation involves the reorganization of photosystem II light-harvesting complexes in the grana membranes of spinach chloroplasts, *Plant Cell* 23 (2011) 1468–1479, <http://dx.doi.org/10.1105/tpc.110.081646>.
- [57] C. Six, J.C. Thomas, L. Garczarek, M. Ostrowski, A. Dufresne, N. Blot, D.J. Scanlan, F. Partensky, Diversity and evolution of phycobilisomes in marine *Synechococcus* spp.: a comparative genomics study, *Genome Biol.* 8 (2007) R259, <http://dx.doi.org/10.1186/gb-2007-8-12-r259>.